

This is 0.75 at  $J=10$ , 0.9 at  $J=20$ . The other crossing coefficients are much closer to 1 at  $J=10$ . Roughly then, the  $J$ -independent bootstrap solution (12) evolves for  $J \geq 10$ . Of course, bootstrap solutions may be found at lower  $J$  which are not the simple ones given in (10)–(12).

(4) A reasonable parametrization of the actual  $\rho$ - $A_2$  trajectory is  $J \simeq 0.5 + m^2$ , with  $m$  in GeV. A readily verified consequence is that the decay modes  $\rho^J \rightarrow A_2^{J-1} + \pi$  or  $A_2^{J+1} \rightarrow \rho^J + \pi$  become energetically impossible for  $J > 12$ . If, however, our result for high  $J$ ,  $g(\rho^J \rightarrow A_2^{J-1} + \pi) = g(A_2^{J+1} \rightarrow \rho^J + \pi)$ , continues to

maintain approximate validity for  $J$  between 5 and 10, and if the initial stage in the decay of  $\rho^J(A_2^{J+1})$  is  $\rho^J \rightarrow A_2^{J-1} + \pi(A_2^{J+1} \rightarrow \rho^J + \pi)$ , then the approximate equality of the widths ( $\simeq 20$  MeV) of the resonance observed in the mass-spectrometer data<sup>2</sup> could be understood as a consequence of the model.

We are aware of many of the shortcomings of the present approach, such as the lack of prediction of a mass formula or the lack of results for small  $J$ . Nevertheless, we feel that the model has provided a simple and transparent dynamical approach to Mandelstam's hypothesis<sup>3</sup> as applied to the  $\rho$ - $A_2$  system.

## Large-Angle Proton-Proton Scattering and the Pomeranchuk Trajectory\*†

KERSON HUANG AND STEPHEN PINSKY

*Laboratory for Nuclear Science and Department of Physics, Massachusetts Institute of Technology,  
Cambridge, Massachusetts 02139*

(Received 27 May 1968)

Proton-proton scattering at large momentum transfers is analyzed in detail, with spin and the Pauli principle taken into account. It is pointed out that various empirical formulas that fit the gross feature of the data in the neighborhood of  $90^\circ$  c.m. scattering angle are essentially consequences of the Pauli principle. From the data we directly determine the effective Regge trajectory. Two different trajectories seem to dominate different ranges of momentum transfer, and the switchover from one to the other happens almost discontinuously. The trajectories are consistent with  $1+0.5t$  and  $1+0.25t$ , respectively. This supports an earlier model proposed by Huang, Jones, and Teplitz, who suggested that the two trajectories correspond to the Pomeranchuk trajectory and a Regge cut generated by it. Assuming this interpretation, we deduce some properties of the Pomeranchuk trajectory. The differential cross section for  $pp$  scattering at large momentum transfers is fitted in detail, using this model. Consequences for polarization in  $pp$  scattering and the cross sections for  $p\bar{p}$  scattering are also discussed.

### 1. INTRODUCTION

THIS paper contains a detailed analysis of  $pp$  scattering at large momentum transfers, based on an idea proposed by Huang, Jones, and Teplitz.<sup>1</sup> They suggested that, from the point of view of a Regge analysis, scattering at large momentum transfers may be simpler than diffraction scattering, because the Pomeranchuk trajectory  $P$ , which is thought to have a smaller slope than all other Regge-pole trajectories, could dominate the scattering.

Despite the unique position that  $P$  is supposed to have as the leading trajectory, there is a woeful lack of direct experimental evidence for it. A possible reason (apart from the possibility that it may not exist) is that most scattering data pertain to the diffraction region, where other trajectories are also important. It is not

surprising, therefore, that the parameters of  $P$  obtained from fits to diffraction scattering depend sensitively on assumptions made about the forms of residue functions for  $P$ , as well as for other contributing trajectories. Various fits<sup>2</sup> of this type yield different values for the slope of  $P$ , and they spread over the range 0.1–0.5  $(\text{BeV}/c)^{-2}$ . This indicates that if  $P$  exists, its slope is probably less than 1  $(\text{BeV}/c)^{-2}$ , the approximate common slope of all other known trajectories. It seems reasonable to suppose that if  $P$  exists, it will eventually dominate all other trajectories at large momentum transfers. In Ref. 1 this idea was proposed and tested in  $pp$  scattering at  $\theta = 90^\circ$ , where  $\theta$  is the c.m. scattering angle.

There are, however, complications anticipated by the theory. Whenever  $P$  can be exchanged in a scattering process, the simultaneous exchanges of two or more  $P$ 's are also possible. These exchange processes lead to Regge cuts (referred to as the  $P$ - $P$  cut, the  $P$ - $P$ - $P$  cut, etc.) whose branch points have trajectories that lie

\* Work supported in part by the U. S. Atomic Energy Commission under Contract No. AT(30-1)2098.

† Part of this work is contained in a thesis, submitted by S. Pinsky to the Physics Department, M.I.T., in partial fulfillment of the requirements for the Ph.D. degree.

<sup>1</sup> K. Huang, C. E. Jones, and V. L. Teplitz, Phys. Rev. Letters 18, 146 (1967).

<sup>2</sup> W. Rarita, R. J. Riddell, C. B. Chiu, and R. J. N. Phillips, Phys. Rev. 165, 1615 (1968), and references therein.

successively higher.<sup>3</sup> It was assumed in Ref. 1 that these cuts have very small effective coupling compared to that of  $P$ , so that they are unimportant for a certain intermediate range of momentum transfers; but eventually, at sufficiently large momentum transfer,  $P$ - $P$  must dominate over  $P$ , and at still larger momentum transfer higher cuts must also enter.

A particularly dramatic possibility is that the relative coupling constants are such that the switchover from  $P$  to  $P$ - $P$  takes place near a nonsense wrong-signature point of  $P$ . If the residue function of  $P$  has no pole at that point, then the contribution of  $P$  must vanish, and the switchover would occur almost discontinuously. In Ref. 1 this point was chosen for simplicity to be the first nonsense wrong-signature point ( $\alpha = -1$ ) and the sharp break in the experimental cross section observed by Akerlof *et al.*<sup>4</sup> was reproduced at the right place by choosing  $\alpha' = 0.3$  (BeV/c)<sup>-2</sup>.

The analysis of Ref. 1 is only qualitative in that the protons were taken to be spinless. For scattering at  $\theta \neq 90^\circ$ , it becomes essential to take spin into account in order to have the proper symmetries required by the Pauli principle. In this paper, we take full account of spin and the Pauli principle, and will thus be able to compare theoretical results with the vast amount of excellent data at a wide range of angles that has since become available.<sup>5-8</sup> Our results support the basic validity of the picture proposed in Ref. 1, and suggest that the  $P$  trajectory and the cuts generated by it do exist. A summary of the contents of the paper is as follows.

The tedious, but necessary, preliminaries are given in Secs. 2-5. It is noted that the Pauli principle requires a "conspiracy" of Regge singularities in a crossed channel, and we give a practical recipe to deal with it.

In Sec. 6, we show that as a consequence of the Pauli principle, the differential cross section near  $\theta = 90^\circ$  has the property

$$\left[ \frac{d}{d \sin \theta} \left( \ln \frac{d\sigma}{d\Omega} \right) \right]_{\theta=90^\circ} = -f(k),$$

<sup>3</sup> D. Amati, S. Fubini, and A. Stanghellini, *Phys. Letters* **1**, 29 (1962); S. Mandelstam, *Nuovo Cimento* **30**, 1127, (1963); **30**, 1148 (1963).

<sup>4</sup> C. W. Akerlof, R. H. Hieber, A. D. Krisch, K. W. Edwards, L. G. Ratner, and K. Ruddick, *Phys. Rev. Letters* **17**, 1105 (1966); *Phys. Rev.*, **159**, 1138 (1967).

<sup>5</sup> A. R. Clyde, Ph.D. thesis, University of California, Berkeley, 1966 (unpublished).

<sup>6</sup> C. M. Ankenbrandt, University of California Report No. UCRL-17257 (unpublished). C. M. Ankenbrandt, A. R. Clark, B. Cork, T. Elioff, L. T. Kerth, and W. A. Wenzel, *Phys. Rev.* **170**, 1223 (1968).

<sup>7</sup> J. V. Allaby, G. Bellettini, G. Cocconi, A. N. Diddens, M. L. Good, G. Matthiae, E. J. Sacharidis, A. Silverman, and A. M. Wetherell, *Phys. Letters* **23**, 389 (1966); J. V. Allaby, G. Cocconi, A. N. Diddens, A. Klovning, G. Matthiae, E. J. Sacharidis, and A. M. Wetherell, *ibid.* **25B**, 156 (1967).

<sup>8</sup> J. V. Allaby, A. D. Diddens, A. Klovning, E. Littethun, E. J. Sacharidis, K. Schlüpmann, and A. M. Wetherell, in CERN Topical Conference on High-Energy Collisions of Hadrons, 1968 (unpublished).

where  $f(k)$  is finite, and is generally a rapidly increasing function of the c.m. momentum  $k$ . In contrast, this quantity is expected to be infinite for nonidentical particle scattering such as  $\pi p$  and  $p\bar{p}$ . In view of this, it is perhaps not surprising that in  $p\bar{p}$  scattering, empirical formulas of the forms<sup>9,10</sup>

$$\frac{d\sigma}{d\Omega} \propto \exp(-Ak \sin \theta), \quad (\text{Orear, Ref. 9})$$

$$\exp(-A'k^2 \sin^2 \theta), \quad (\text{Krisch, Ref. 10})$$

$$\exp(-A''(k^2 + m^2) \sin \theta), \quad (\text{Allaby } et al., \text{ Ref. 7})$$

can account for the gross behavior of  $d\sigma/d\Omega$  near  $\theta = 90^\circ$ . A more refined empirical formula proposed by Krisch,<sup>11</sup> which decomposes the differential cross section into two terms,

$$d\sigma/d\Omega = (d\sigma^+/d\Omega)_{\text{forward}} + (d\sigma^+/d\Omega)_{\text{backward}},$$

bears a certain similarity to the Regge formula that we derive in Sec. 4 [Eq. (49)]. None of the above forms, however, agrees with the data in detail.

We start the main part of the investigation by first giving a direct experimental test of the hypothesis that, at large  $-t$ ,  $p\bar{p}$  scattering is dominated by a single Regge trajectory. Analyzing the data in a special way, we show in Sec. 6 that there appears to be two different ranges of  $-t$  in which a single trajectory dominates. The dominating trajectory is different for the two ranges, and the switchover from one to the other occurs almost discontinuously. This gives direct support to the picture of Huang, Teplitz, and Jones, in which the two dominating trajectories are  $P$  and the  $P$ - $P$  cut. From the data we can draw the following conclusions, which do not depend sensitively on the choice of residue functions:

(a) The trajectory of  $P$  is consistent with a straight line of slope about 0.5 (BeV/c)<sup>-2</sup>.

(b) The  $P$ - $P$  cut, which has half the slope of  $P$ , exists.

(c) Some or all of the residue functions of  $P$  have fixed poles at  $\alpha = -1$ , of the type pointed out by Jones and Teplitz and by Mandelstam and Wang.<sup>12</sup> There appears to be no fixed pole at  $\alpha = -3$ . The break in the cross section first observed by the Argonne group<sup>4</sup> is attributed to the fact that  $P$  passes through  $\alpha = -3$ .

The main difference between these results and those of Ref. 1 is that  $P$  is found to have a larger slope than thought, so that the relevant nonsense wrong-signature point is now  $\alpha = -3$ , instead of  $\alpha = -1$ .

We fit the differential cross section in detail in Sec. 7. The model makes use of three trajectories:  $P$ ,  $P$ - $P$ ,

<sup>9</sup> J. Orear, *Phys. Rev. Letters* **12**, 112 (1964).

<sup>10</sup> A. D. Krisch, *Phys. Rev. Letters* **11**, 217 (1963).

<sup>11</sup> A. D. Krisch, *Phys. Rev. Letters* **19**, 1149 (1967).

<sup>12</sup> C. E. Jones and V. L. Teplitz, *Phys. Rev.* **159**, 1271 (1967); S. Mandelstam and L. L. Wang, *ibid.* **160**, 1490 (1967); see also A. H. Mueller and T. L. Trueman, *ibid.* **160**, 1296 (1967).

and  $P$ - $P$ - $P$ . There are eight free parameters, which are adjusted by a  $\chi^2$  fit to 97 selected data points. The final theoretical cross section agrees reasonably well with all the data available in the range

$$\begin{aligned} 5 < p_{\text{lab}} < 26 \text{ BeV}/c, \\ 3 < -t < 18 (\text{BeV}/c)^2, \end{aligned}$$

consisting of some 200 data points. The latest measurements from the CERN group,<sup>8</sup> consisting of 86 data points, have not been used in our fit. They agree with our theoretical curves in shape but not in absolute magnitudes. We note that they differ significantly from earlier measurements from the same laboratory<sup>7</sup> in absolute normalization.

Predictions on polarization in  $p\bar{p}$  scattering and on the differential cross section of  $p\bar{p}$  scattering are made in Sec. 7.

Finally, some theoretical speculations on extremely high-energy phenomena are given in Sec. 8.

## 2. PAULI PRINCIPLE

We define, as usual,

$$\begin{aligned} s &= 4(k^2 + m^2), \\ t &= -2k^2(1 - z), \\ u &= -2k^2(1 + z), \end{aligned} \quad (1)$$

where  $k$  and  $z = \cos\theta$  are, respectively, the momentum and the cosine of the scattering angle in the c.m. system, and  $m$  is the proton mass. The corresponding quantities for the  $t$ - and  $u$ -channel reactions will be distinguished by an appropriate subscript:

$$\begin{aligned} k_t^2 &= -m^2 + \frac{1}{4}t, \\ z_t &= 1 - 2s/(4m^2 - t), \\ k_u^2 &= -m^2 + \frac{1}{4}u, \\ z_u &= 1 - 2s/(4m^2 - u). \end{aligned} \quad (2)$$

There are 16 helicity amplitudes<sup>13</sup>  $f_{cd,ab^s}(s,t)$ , where the helicity indices  $c, d, a, b$ , independently take on the values  $+$  and  $-$ . They are so normalized that the unpolarized differential cross section is given by

$$\frac{d\sigma}{d\Omega} = (16\pi^2 s)^{-1} \sum_{a,b,c,d} |f_{cd,ab^s}(s,t)|^2. \quad (3)$$

Owing to the conservation of parity, total spin, and the invariance under time reversal,<sup>14</sup> only five helicity amplitudes are independent, and are taken to be

$$\begin{aligned} f_1^s &= f_{++,++^s}, & f_2^s &= f_{+,-,-^s}, \\ f_3^s &= f_{+,-,+^s}, & f_4^s &= f_{+,-,+^s}, \\ f_5^s &= f_{+,-,+^s}. \end{aligned} \quad (4)$$

<sup>13</sup> M. Jacob and G. C. Wick, Ann. Phys. (N. Y.) **1**, 404 (1959). Our helicity amplitudes are theirs multiplied by  $(16\pi^2 s)^{1/2}$ .

<sup>14</sup> M. L. Goldberger, M. J. Grisaru, S. W. MacDowell, and D. Y. Wong, Phys. Rev. **120**, 2250 (1960).

TABLE I. Relations among the helicity amplitudes,  $f_{cd,ab^s} \equiv (cd,ab)$ .

Independent amplitude	Equal to
( $++$ , $++$ )	( $--$ , $--$ ).
( $++$ , $--$ )	( $--$ , $++$ ).
( $+-$ , $+-$ )	( $-+$ , $-+$ ).
( $+-$ , $-+$ )	( $-+$ , $+-$ ).
( $++$ , $+-$ )	( $--$ , $+-$ ), ( $-+$ , $--$ ), ( $-+$ , $++$ ), ( $--$ , $-+$ ), ( $++$ , $-+$ ), ( $+-$ , $++$ ), ( $-+$ , $--$ ).

All others are related to one of the above as indicated in Table I. For convenience, let  $f^s(s,t)$  denote the column vector whose components are  $f_1^s, \dots, f_5^s$ . Then

$$d\sigma/d\Omega = (8\pi^2 s)^{-1} (|f_1^s|^2 + |f_2^s|^2 + |f_3^s|^2 + |f_4^s|^2 + 4|f_5^s|^2). \quad (5)$$

It can be shown that the Pauli principle imposes on  $f^s(s,t)$  the requirement

$$f^s(s,u) = \mathcal{R} f^s(s,t), \quad (6)$$

where  $\mathcal{R}$  is a  $5 \times 5$  matrix with  $\mathcal{R}^2 = 1$ :

$$\mathcal{R} = \begin{pmatrix} 1 & 0 & 0 & 0 & 0 \\ 0 & 1 & 0 & 0 & 0 \\ 0 & 0 & 0 & -1 & 0 \\ 0 & 0 & -1 & 0 & 0 \\ 0 & 0 & 0 & 0 & -1 \end{pmatrix}. \quad (7)$$

At  $\theta = 90^\circ$  we must have  $f_3^s + f_4^s = 0$ , and  $f_5^s = 0$ , leaving only three nonvanishing independent amplitudes.

The helicity amplitudes for the  $t$ -channel reaction  $p\bar{p} \rightarrow p\bar{p}$  are denoted by  $f_{cA,Db^t}(s,t)$ , where capital subscripts refer to the helicities of antiprotons. Thus  $f_{cA,Db^t}(s,t)$  is the helicity amplitude for  $p\bar{p} \rightarrow p\bar{p}$ , with total c.m. energy squared equal to  $t$ , and invariant momentum transfer squared equal to  $s$ . We define the  $u$ -channel helicity amplitude  $f_{cA,Db^u}(s,t)$  by an identical statement except that the total c.m. energy squared is  $u$ :

$$f_{cA,Db^u}(s,t) = f_{cA,Db^t}(s,u). \quad (8)$$

The crossing relation between  $f_{cA,Db^t}$  and  $f_{cd,ab^s}$  is<sup>15</sup>

$$f_{cd,ab^s}(s,t) = \sum_{c',A',D',b'} d_{A'a}^{1/2}(\chi_t) d_{b'b'}^{1/2}(\pi - \chi_t) \times d_{c'c}^{1/2}(\pi - \chi_t) d_{D'd}^{1/2}(\chi_t) f_{c'A',D'b'^t}(s,t), \quad (9)$$

where

$$d_{\lambda\mu}^{1/2}(\theta) = \begin{pmatrix} \cos\frac{1}{2}\theta & -\sin\frac{1}{2}\theta \\ \sin\frac{1}{2}\theta & \cos\frac{1}{2}\theta \end{pmatrix}, \quad (10)$$

$$\cos\chi_t = [st/(s - 4m^2)(t - 4m^2)]^{1/2}. \quad (11)$$

There are again five independent  $t$ -channel helicity amplitudes, taken to be  $f_1^t, \dots, f_5^t$ , which are defined

<sup>15</sup> T. L. Trueman and G. C. Wick, Ann. Phys. (N. Y.) **26**, 322 (1964).

by the analog of (4). Table I applies also to the  $t$ -channel amplitudes. Denoting by  $f^t(s,t)$  the column vector whose components are  $f_1^t, \dots, f_5^t$ , we deduce from (9), after a straightforward calculation, that

$$f(s,t)^s = \mathfrak{N}(st)f(s,t)^t, \quad (12)$$

where

$$\mathfrak{N}(st) = \frac{1}{2} \sin^2 \chi_t \begin{pmatrix} 1 & 1 & 1 & a & 4b \\ 1 & -a & 1 & -1 & 4b \\ 1 & 1 & -a & -1 & 4b \\ a & -1 & -1 & 1 & -4b \\ -b & -b & -b & b & 2(1-b^2) \end{pmatrix}, \quad (13)$$

$$a = 2 \csc^2 \chi_t - 1, \quad b = \cot \chi_t. \quad (14)$$

The  $s$ - $u$  crossing relation follows from (12), (8), and (6):

$$f^s(s,t) = \mathfrak{R}\mathfrak{N}(s,u)f^u(s,t). \quad (15)$$

Comparison between (15) and (12) yields the  $t$ - $u$  crossing relation:

$$f^t(s,t) = \mathfrak{N}^{-1}(st)\mathfrak{R}\mathfrak{N}(s,u)f^u(s,t). \quad (16)$$

Using (8) again, we convert this to

$$f^t(s,t) = \mathfrak{N}^{-1}(st)\mathfrak{R}\mathfrak{N}(s,u)f^t(s,u), \quad (17)$$

which is the Pauli principle stated in terms of  $t$ -channel helicity amplitudes. It is important to note that (12) and (15) are completely equivalent if  $f^t$  and  $f^u$  are the exact helicity amplitudes. In an approximate calculation, we must maintain this equivalence in order to preserve the Pauli principle. One way to do this is to insure that (17) is satisfied.

Let us examine the implication of (17) for Regge poles. A Regge pole in the  $t$ -channel is a pole in the complex angular-momentum plane of the partial-wave amplitudes of the  $t$  channel. Its contribution to  $f^t$ , through the Sommerfeld-Watson transformation, can be uniquely isolated from contributions from other poles, cuts, and "background terms," and has the general form

$$f(st) = \beta(t)Q_{-\alpha(t)-1}(-z_t)(1 \pm e^{-i\pi\alpha(t)})/\cos\pi\alpha(t),$$

where  $Q_J$  is a Legendre function of the second kind, and spin complications have been ignored for the present purpose. The functions  $\alpha(t)$  and  $\beta(t)$  are arbitrary, but whatever they are  $f(s,t)$  cannot satisfy (17). We therefore conclude that whenever a Regge pole occurs it must be accompanied by other singularities that conspire with the Regge pole to satisfy the Pauli principle.<sup>16</sup> That is, there must always be additional additive contributions to  $f(s,t)$ . We shall not inquire into the detailed nature of the conspiring singularities,<sup>17</sup> but merely note the obvious fact that they reflect the existence of the same Regge pole in the  $u$  channel. It is therefore intuitively suggested that the conspiring

<sup>16</sup> Symmetry in a given channel generally requires a conspiracy of Regge singularities in a crossed channel. The more familiar type of conspiracy arises from the conservation of angular momentum.

<sup>17</sup> They could consist of an infinite family of poles.

singularities are precisely the crossed effects of the  $u$ -channel Regge pole, with the crossing governed by (16). This is expressed more precisely by the following recipe. Let

$$\tilde{f}^t(s,t) = \text{contribution of a } t\text{-channel Regge pole to } f^t(s,t). \quad (18)$$

The contribution of the same Regge pole in the  $u$  channel to  $f^u(s,t)$  is then  $\tilde{f}^u(s,t)$ , which, when crossed over to the  $t$  channel according to (16) and (8), gives  $\mathfrak{N}^{-1}(s,t)\mathfrak{R}\mathfrak{N}(s,u)\tilde{f}^u(s,t)$ . The complete contribution associated with a given Regge pole is taken to be

$$f_{\text{pole}}^t(s,t) = \tilde{f}^t(s,t) + \mathfrak{N}^{-1}(st)\mathfrak{R}\mathfrak{N}(s,u)\tilde{f}^u(s,u). \quad (19)$$

Clearly this satisfies (17) identically. Substitution of (19) into (12) yields the contribution to  $f^s(s,t)$  associated with a given Regge pole:

$$f_{\text{pole}}^s(st) = \mathfrak{N}(st)\tilde{f}^t(s,t) + \mathfrak{R}\mathfrak{N}(s,u)\tilde{f}^u(s,u), \quad (20)$$

which satisfies (6) identically. The recipe can also be used for a Regge cut. In general, the second term of (20) is negligible in the diffraction region ( $\theta \rightarrow 0$ ), but it becomes comparable to the first term as  $\theta \rightarrow 90^\circ$ .

Since the recipe (20) has not been proven, the question arises whether we have counted the same Regge pole twice. We have learned<sup>18</sup> in the case of pion-nucleon scattering that a simple addition of Regge poles in the  $t$  channel to those in the  $s$  channel (direct-channel resonances) is incorrect, for the result is inconsistent with analyticity. We believe that no double counting is involved in the present case, for (20) does not represent a simple addition of  $t$ - and  $u$ -channel Regge poles, but the relative amounts of  $t$ - and  $u$ -channel contributions are uniquely determined by the Pauli principle. A preliminary study of the consistency of (20) with finite-energy sum rules<sup>18</sup> reveals no inconsistencies. This analysis is in progress and the results will be published separately in due time.

As an indication for the validity of the recipe (20), we may compare  $p\bar{p}$  scattering with  $p\bar{p}$  scattering at  $\theta = 90^\circ$ . The latter differs from the former only by a charge conjugation of either the initial or final state in the  $t$  channel. A Regge trajectory even (odd) under charge conjugation makes the same contribution to the two processes with the same (opposite) sign. Since the Pauli principle does not apply in  $p\bar{p}$  scattering, a  $t$ -channel Regge pole need not be accompanied by conspiring singularities. This means that the conspiring singularities in  $p\bar{p}$  scattering must consist of singularities of both signatures under charge conjugation, so that they add for  $p\bar{p}$  and cancel for  $p\bar{p}$ . The  $u$  channel of  $p\bar{p}$  scattering is different from that of  $p\bar{p}$  scattering in that it has baryon number 2 instead of 0. Although there is no known Regge trajectory of baryon number 2,

<sup>18</sup> R. Dolen, D. Horn, and C. Schmid, Phys. Rev. **166**, 1768 (1968).

a cut may be coupled to the  $u$  channel, e.g., the nucleon-nucleon cut, which we neglect.

Suppose (20) were incorrect, and that somehow the  $t$ -channel Regge pole alone can be so arranged as to satisfy the Pauli principle, at least near  $\theta=90^\circ$ . (We have seen that this is impossible for all  $\theta$ .) Then, if a single trajectory dominates the scattering, we would expect that  $p\bar{p}$  and  $p\bar{p}$  have the same cross section at  $\theta=90^\circ$ . Experimentally,<sup>4,19</sup> however, the  $p\bar{p}$  cross section at  $p_{\text{lab}}=5.9$  BeV/ $c$  and  $\theta=90^\circ$  is greater than that of  $p\bar{p}$  at least by a factor of 10. This indicates that there are additional contributions (which we attribute to the  $u$  channel) present in  $p\bar{p}$  but not in  $p\bar{p}$ . In Sec. 5 C we point out that the assumption of single-trajectory dominance is justified, and make an absolute calculation of the  $p\bar{p}$  section using parameters determined by fitting the  $p\bar{p}$  cross section based on the recipe (20). The right magnitude of the  $p\bar{p}$  cross section is obtained where the experimental statistics are good. At  $\theta=90^\circ$ , where statistics are poor, the theoretical prediction seems to be too large by a factor of 2-3. The discrepancy may be accounted for by other effects, such as a cut in the  $u$  channel.

### 3. PARTIAL-WAVE AMPLITUDES

We define  $t$ -channel partial-wave amplitudes by the decomposition

$$f_{cA,Db^t}(st) = \sum_J (2J+1) \langle cA | G^J(t) | Db \rangle d_{\lambda\mu}^J(z_t), \quad (21)$$

$$\lambda = D - b, \quad \mu = c - A,$$

where  $d_{\lambda\mu}^J(z_t)$  are the usual rotation coefficients.<sup>18</sup> For a given  $J$ , the four independent helicity states  $|++\rangle$ ,  $|--\rangle$ ,  $|+-\rangle$ , and  $| - + \rangle$  can be recombined to form four eigenstates of parity<sup>20</sup>:

$$\begin{aligned} |0-\rangle &= 2^{-1/2}(|++\rangle - |--\rangle), \\ |0+\rangle &= 2^{-1/2}(|++\rangle + |--\rangle), \\ |1+\rangle &= 2^{-1/2}(|+-\rangle + |-+\rangle), \\ |1-\rangle &= 2^{-1/2}(|+-\rangle - |-+\rangle), \end{aligned} \quad (22)$$

where, in the symbol  $|\lambda\pm\rangle$ ,  $\lambda$  stands for the total angular momentum along the direction of relative momentum, and  $\pm$  corresponds to the eigenvalue of parity  $\pm(-)^J$ . Table II gives the conserved quantum numbers for these states and the known Regge trajectories coupled to them. The only nonvanishing off-diagonal transition matrix element is that between  $|0+\rangle$  and  $|1+\rangle$ . We can define five new partial-wave amplitudes with definite parity, denoted by  $G_{\lambda\mu}^{J\pm}(t)$ ,<sup>21</sup>

<sup>19</sup> J. Orear (private communication); A. Ashmore, C. J. S. Damerell, W. R. Frisken, R. Rubenstein, J. Orear, D. P. Owen, F. C. Peterson, A. L. Read, D. G. Ryan, and D. H. White, Phys. Rev. Letters **21**, 387 (1968).

<sup>20</sup> M. Geil-Mann, M. L. Goldberger, F. E. Low, E. Marx, and F. Zachariasen, Phys. Rev. **133**, B145 (1964).

<sup>21</sup> They are related to the amplitudes of Ref. 14 by  $G_{00}^{J-} = f_0^J$ ,  $G_{11}^{J-} = f_1^J$ ,  $G_{00}^{J+} = f_{11}^J$ ,  $G_{11}^{J+} = f_{22}^J$ ,  $G_{10}^{J+} = f_{12}^J$ .

TABLE II. Helicity states of definite angular momentum and parity.

State	Charge conjugation	Parity	Total spin	Trajectory
$ 0-\rangle$	$(-)^J$	$-(-)^J$	0	$\pi, B(1^+)$
$ 0+\rangle$	$(-)^J$	$(-)^J$	1	$P, P', \rho, \omega, A_2$
$ 1+\rangle$	$(-)^J$	$(-)^J$	1	$P, P', \rho, \omega, A_2$
$ 1-\rangle$	$-(-)^J$	$-(-)^J$	1	$A_1$

and related to the original partial-wave amplitudes by

$$\begin{aligned} \langle ++ | G^J | ++ \rangle &= \frac{1}{2}(G_{00}^{J+} + G_{00}^{J-}), \\ \langle ++ | G^J | -- \rangle &= \frac{1}{2}(G_{00}^{J+} - G_{00}^{J-}), \\ \langle +- | G^J | +- \rangle &= \frac{1}{2}(G_{11}^{J+} + G_{11}^{J-}), \\ \langle +- | G^J | -+ \rangle &= \frac{1}{2}(G_{11}^{J+} - G_{11}^{J-}), \\ \langle ++ | G^J | +- \rangle &= \frac{1}{2}G_{10}^{J+}. \end{aligned} \quad (23)$$

For the purpose of Reggeization, it is convenient to define new helicity amplitudes more directly related to  $G_{\lambda\mu}^{J\pm}$ . Following Ref. 20, we define five  $t$ -channel amplitudes  $g_i(s,t)$ , which are free of kinematic singularities in  $s$ :

$$\begin{aligned} g_1(st) &= \sum_{J=0}^{\infty} (2J+1) G_{00}^{J+}(t) e_{00}^{J+}(z_t), \\ g_2(st) &= \sum_{J=0}^{\infty} (2J+1) G_{00}^{J-}(t) e_{00}^{J+}(z_t), \\ g_3(st) &= \sum_{J=1}^{\infty} (2J+1) [G_{11}^{J+}(t) e_{11}^{J+}(z_t) \\ &\quad + G_{11}^{J-}(t) e_{11}^{J-}(z_t)], \\ g_4(st) &= \sum_{J=1}^{\infty} (2J+1) [G_{11}^{J-}(t) e_{11}^{J+}(z_t) \\ &\quad + G_{11}^{J+}(t) e_{11}^{J-}(z_t)], \\ g_5(st) &= \sum_{J=1}^{\infty} (2J+1) G_{10}^{J+}(t) e_{10}^{J+}(z_t), \end{aligned} \quad (24)$$

with the inverse relations

$$\begin{aligned} G_{00}^{J+}(t) &= \frac{1}{2} \int_{-1}^{+1} dz c_{00}^{J+} g_1, \\ G_{00}^{J-}(t) &= \frac{1}{2} \int_{-1}^{+1} dz c_{00}^{J+} g_2, \\ G_{11}^{J+}(t) &= \frac{1}{2} \int_{-1}^{+1} dz (c_{11}^{J+} g_3 + c_{11}^{J-} g_4), \\ G_{11}^{J-}(t) &= \frac{1}{2} \int_{-1}^{+1} dz (c_{11}^{J+} g_4 + c_{11}^{J-} g_3), \\ G_{10}^{J+}(t) &= \frac{1}{2} \int_{-1}^{+1} dz c_{10}^{J+} g_5, \end{aligned} \quad (25)$$

where under the integrals  $c_{\lambda\mu}^{J\pm} = c_{\lambda\mu}^{J\pm}(z)$ , and  $g_i = g(s(t,z), t)$ , with  $s(t,z) = -2k_i^2(1-z)$ . The functions  $e_{\lambda\mu}^{J\pm}$  and  $c_{\lambda\mu}^{J\pm}$  are defined in Ref. 20, with relevant ones given explicitly below:

$$\begin{aligned} e_{00}^{J+} &= P_J, & e_{00}^{J-} &= 0, \\ e_{11}^{J+} &= [J(J+1)]^{-1}(P_J' + zP_J''), & e_{11}^{J-} &= -[J(J+1)]^{-1}P_J'', \\ e_{10}^{J+} &= -[J(J+1)]^{-1/2}P_J', & e_{10}^{J-} &= 0, \\ c_{00}^{J+} &= P_J, & c_{00}^{J-} &= 0, \\ c_{11}^{J+} &= (2J+1)^{-1}[(J+1)P_{J-1} + JP_{J+1}], & c_{11}^{J-} &= P_J, \\ c_{10}^{J+} &= -(2J+1)^{-1}[J(J+1)]^{1/2}(P_{J-1} - P_{J+1}), & c_{10}^{J-} &= 0, \end{aligned} \quad (26)$$

where  $P_J$  is a Legendre polynomial in  $z$ , and a prime denotes differentiation with respect to  $z$ . In the limit  $z_t \rightarrow \infty$ ,  $e_{\lambda\mu}^{J+}$  dominates over  $e_{\lambda\mu}^{J-}$ , so that  $g_1, g_3$ , and  $g_5$  are dominated by Regge poles of parity  $(-)^J$ , and  $g_2, g_4$  are dominated by those of parity  $-(-)^J$ . The relation between  $g_i$  and  $f^i$  is

$$f^i(s, t) = \mathcal{L}(s, t)g(st), \quad (27)$$

where

$$\mathcal{L}(s, t) = \frac{1}{2} \begin{pmatrix} 1 & 1 & 0 & 0 & 0 \\ 1 & -1 & 0 & 0 & 0 \\ 0 & 0 & 1+z_t & 1+z_t & 0 \\ 0 & 0 & 1-z_t & -1+z_t & 0 \\ 0 & 0 & 0 & 0 & i(z_t^2-1)^{1/2} \end{pmatrix}. \quad (28)$$

The amplitudes  $g_i(s, t)$  have no kinematic singularities in  $s$ , but they still have kinematic singularities in  $t$ . The latter can be isolated<sup>14,22</sup> by putting

$$\begin{aligned} g_1 &= k_t^{-2}\bar{g}_1, & g_2 &= k_t^{-2}\bar{g}_2, \\ g_3 &= \bar{g}_3, & g_4 &= \bar{g}_4, \\ g_5 &= t^{1/2}\bar{g}_5. \end{aligned} \quad (29)$$

Then  $\bar{g}_i(s, t)$  are free of kinematic singularities in both  $s$  and  $t$ , and we assume that they have Mandelstam representations. When  $\bar{g}_i$  is substituted in place of  $g_i$  in (25), the resulting partial-wave amplitudes have Gribov-Froissart representation similar to those for the scattering of spinless particles, i.e., they are linear combinations of terms of the form  $\int dz A(t, z)Q_{J\pm 1}(z)$ , where  $Q_J(z)$  is a Legendre function of the second kind. The continuation into the complex  $J$  plane, and the introduction of signature, proceeds in a manner analogous to the spinless case. Assuming the convergence of the Gribov-Froissart integrals, we have the Mandelstam symmetry<sup>23</sup>

$$G_{\lambda\mu}^{J\pm}(t) = G_{\lambda\mu}^{(-J-1)\pm}(t) \quad \text{for } J = \text{half-integer}, \quad (30)$$

which follows from the fact that  $Q_J(z) = Q_{-J-1}(z)$  at half-integer values of  $J$ . We further have<sup>24</sup>

$$G_{11}^{J\pm}(t) = G_{11}^{(-J-1)\mp}(t) \quad \text{for } J = 0, -1. \quad (31)$$

As discussed in the Appendix, these symmetries give rise to possible compensating trajectories, but we shall

not make use of compensating trajectories in later developments.

#### 4. REGGE POLES

We consider only the three partial-wave amplitudes to which the  $P$  trajectory can be coupled:  $G_{00}^{J+}(t)$ ,  $G_{11}^{J+}(t)$ , and  $G_{10}^{J+}(t)$ . When continued into the  $J$  plane, each of these give rise to two signed amplitudes, which coincide with  $G_{\lambda\mu}^{J+}(t)$  at  $J = \text{even}$  or  $\text{odd}$  integer, respectively. To avoid a profusion of superscripts, we denote the continued amplitudes of definite signature (even or odd) simply by  $G_{00}(J, t)$ ,  $G_{11}(J, t)$ , and  $G_{10}(J, t)$ . The  $P$  trajectory is coupled to the even-signed amplitudes.

A Regge pole at  $J = \alpha(t)$ , of parity  $(-)^J$  and of given signature, occurs in the form

$$G_{\lambda\mu}(J, t) = \frac{\beta_{\lambda\mu}(t)}{J - \alpha(t)} + R_{\lambda\mu}(J, t), \quad (32)$$

where  $R_{\lambda\mu}(J, t)$  contains other singularities in the  $J$  plane, in particular those necessary to satisfy the Pauli principle, as discussed in Sec. 3. For practical purposes, we ignore singularities of the latter type, for their effects can be taken into account through the use of the recipe (20), as explained earlier.

From (25) and (26), it is seen that  $G_{10}(J, t)$  contains kinematic branch cuts through a factor of  $[J(J+1)]^{1/2}$ . As functions of  $t$ ,  $G_{\lambda\mu}(J, t)$  have threshold branch cuts at  $k_t^2 = 0$ , which can be removed by dividing the amplitudes by  $k_t^{2J}$ .<sup>25</sup> The functions  $\alpha(t)$  and  $\beta_{\lambda\mu}(t)$  have no left-hand cuts in  $t$ , and are therefore real for  $t < 4\mu^2$ .<sup>26</sup> Through the use of two-body unitarity one can show<sup>27</sup> that for  $4\mu^2 < t < 16\mu^2$ , where  $\mu$  is the pion mass,

$$\beta_{00}(t)\beta_{11}(t) = [\beta_{10}(t)]^2. \quad (33)$$

This relation is assumed to hold for all  $t$ .

To take into account all the properties described above, together with the kinematic singularities in  $t$

<sup>25</sup> See, e.g., E. J. Squires, *Complex Angular Momenta and Particle Physics* (W. A. Benjamin, Inc., New York, 1964), p. 46.

<sup>26</sup> A. O. Barut and D. Zwanziger, *Phys. Rev.* **127**, 974 (1962); R. Oehme and G. Tiktopoulos, *Phys. Letters* **2**, 86 (1962).

<sup>27</sup> V. N. Gribov and I. Ya. Pomeranchuk, *Phys. Rev. Letters* **8**, 343 (1962).

<sup>22</sup> L. L. Wang, *Phys. Rev.* **142**, 1187 (1966).

<sup>23</sup> S. Mandelstam, *Ann. Phys.* (N. Y.) **19**, 254 (1962).

<sup>24</sup> See Ref. 20, Eq. (B16).

displayed in (29), we write

$$\begin{aligned}\beta_{00}(t) &= (k_t^2/s_1)^{\alpha-1}\alpha\lambda_0, \\ \beta_{11}(t) &= (k_t^2/s_1)^{\alpha-1}t(\alpha+1)\lambda_1, \\ \beta_{10}(t) &= \pm(k_t^2/s_1)^{\alpha-1}t^{1/2}[\alpha(\alpha+1)]^{1/2}(\lambda_1\lambda_0)^{1/2},\end{aligned}\quad (34)$$

where  $s_1$  is an arbitrary scale. For  $t < 4\mu^2$ ,  $\lambda_0$  and  $\lambda_1$  are real functions of  $t$  having the same sign:

$$\lambda_1\lambda_0 \geq 0. \quad (35)$$

The respective factors  $\alpha$  and  $1+\alpha$  in  $\beta_{00}$  and  $\beta_{11}$  and the factor  $t$  in  $\beta_{11}$  are introduced here merely as a convenient way to satisfy the factorization property. They could be removed by poles in  $\lambda_0$  and  $\lambda_1$ . For the  $P$  trajectory the factor  $t$  in  $\beta_{11}$  should be present, and expresses the fact that at  $t=0$  the trajectory chooses evasion rather than conspiracy. Possible zeros and poles in  $\lambda_0$  and  $\lambda_1$  depend on the choice of "compensation" mechanisms discussed more fully in the Appendix.

The process of Reggeization consists of converting the sums in (24) into Watson-Sommerfeld integrals, and of evaluating the contributions from singularities in the complex  $J$  plane. Following the procedure of Ref. 20, in which the Mandelstam symmetry (30) enables us to push the "background integral" sufficiently far to the left as to be negligible, we find that the contributions from the pole term of (32), corresponding to a Regge pole of parity  $(-)^J$  and signature  $\eta$ , are given by

$$\begin{aligned}g_1(st) &= -\beta_{00}(t)\xi(t)E_{00}^{\alpha+}(-z_t), \\ g_2(st) &= 0, \\ g_3(st) &= \beta_{11}(t)\xi(t)E_{11}^{\alpha+}(-z_t), \\ g_4(st) &= -\beta_{11}(t)\xi(t)E_{11}^{\alpha-}(-z_t), \\ g_5(st) &= \beta_{10}(t)\xi(t)E_{10}^{\alpha+}(-z_t),\end{aligned}\quad (36)$$

where

$$\xi(t) = \pi(\alpha + \frac{1}{2})(1 + \eta e^{-i\pi\alpha})/\sin\pi\alpha. \quad (37)$$

The function  $E_{\lambda\mu}^{\alpha\pm}(z)$  is obtained from  $e_{\lambda\mu}^{\alpha\pm}(z)$  of (26) by replacing  $P_\alpha(z)$  with

$$\begin{aligned}\mathcal{P}_\alpha(z) &= -(\pi^{-1}\tan\pi\alpha)Q_{-\alpha-1}(z) \\ &= \pi^{-1/2}[\Gamma(\alpha + \frac{1}{2})/\Gamma(\alpha + 1)](2z)^\alpha \\ &\quad \times F(-\frac{1}{2}\alpha, \frac{1}{2} - \frac{1}{2}\alpha; \frac{1}{2} - \alpha; z^{-2}).\end{aligned}\quad (38)$$

Explicit formulas for the relevant  $E_{\lambda\mu}^{\alpha\pm}$  are given in the Appendix.

In subsequent developments we expand (36) in inverse powers of  $z_t$  and neglect terms of order  $z_t^{-2}$  in comparison with 1. These terms amount to about 10% corrections, and are not physically significant because they are of the same order as contributions from unknown low-lying trajectories, as discussed in the

Appendix. The formulas we shall use are

$$\begin{aligned}g_1(s,t) &= -\beta_{00}(t)\xi(t)c(\alpha)(-z_t)^{\alpha-1}, \\ g_2(s,t) &= 0, \\ g_3(s,t) &= \beta_{11}(t)\xi(t)[\alpha/(\alpha+1)]c(\alpha)(-z_t)^{\alpha-1}, \\ g_4(s,t) &= \beta_{11}(t)\xi(t)[(\alpha-1)/(\alpha+1)]c(\alpha)(-z_t)^{\alpha-2}, \\ g_5(s,t) &= -\beta_{10}(t)\xi(t)[\alpha/(\alpha+1)]^{1/2}c(\alpha)(-z_t)^{\alpha-2},\end{aligned}\quad (39)$$

where  $\xi(t)$  is defined by (37), and

$$c(\alpha) = 2^\alpha\Gamma(\alpha + \frac{1}{2})/[\pi^{1/2}\Gamma(\alpha + 1)]. \quad (40)$$

To obtain the contribution of a Regge pole to the cross section, the steps are as follows. (a) Obtain the contributions of the pole term of (32) to the amplitudes  $g$  of (24); (b) substitute the result into (27) to obtain  $f^t$ ; (c) substitute  $f^t$  into (20) to obtain  $f_{\text{pole}}^s$ ; and (d) substitute  $f_{\text{pole}}^s$  into (5) to obtain  $d\sigma/d\Omega$ . The treatment of a Regge cut is similar.

Substitution of (39) into (27) yields the simple result

$$\tilde{f}^t(s,t) = A_t \begin{pmatrix} \cos^2\frac{1}{2}\phi_t \\ \cos^2\frac{1}{2}\phi_t \\ -(1 + \alpha_t^{-1}z_t^{-1})\sin^2\frac{1}{2}\phi_t \\ (1 - \alpha_t^{-1}z_t^{-1})\sin^2\frac{1}{2}\phi_t \\ \frac{1}{2}\sin\phi_t \end{pmatrix}, \quad (41)$$

where  $\alpha_t \equiv \alpha(t)$ , and

$$\cos\phi_t = [\lambda_0(t) + t\lambda_1(t)]/[\lambda_0(t) - t\lambda_1(t)], \quad (42)$$

$$\begin{aligned}A_t &= \frac{1}{2}\pi^{1/2}[\lambda_0(t) - t\lambda_1(t)]\Gamma(\alpha_t + \frac{3}{2})\Gamma(1 - \alpha_t) \\ &\quad \times [(s-u)/2s_1]^{\alpha_t}(m^2 - \frac{1}{4}t)^{-1}(e^{-i\pi\alpha_t} + \eta).\end{aligned}\quad (43)$$

The condition (35) guarantees that  $|\cos\phi_t| \leq 1$  for  $t < 0$ . Both signs in front of  $\beta_{10}$  in (34) are covered when  $\phi_t$  varies from 0 to  $2\pi$ . Note that  $\phi_t$  is a function of  $t$  only, but  $A_t$  depends on both  $t$  and  $s$ , with the latter dependence coming solely from the factor  $(s-u)^{\alpha_t}$ . When (41) is substituted into (20), we obtain the single Regge-pole contributions to the  $s$ -channel helicity amplitudes<sup>28</sup>:

$$\begin{aligned}f_1^s(st) &= A_t[\sin^2(\chi_t + \frac{1}{2}\phi_t) - (\alpha_t z_t)^{-1}\sin^2\frac{1}{2}\phi_t] \\ &\quad + A_u[\sin^2(\chi_u + \frac{1}{2}\phi_u) - (\alpha_u z_u)^{-1}\sin^2\frac{1}{2}\phi_u], \\ f_2^s(st) &= -A_t \cos^2(\chi_t + \frac{1}{2}\phi_t) - A_u \cos^2(\chi_u + \frac{1}{2}\phi_u), \\ f_3^s(st) &= A_t[\sin^2(\chi_t + \frac{1}{2}\phi_t) + (\alpha_t z_t)^{-1}\sin^2\frac{1}{2}\phi_t] \\ &\quad - A_u \cos^2(\chi_u + \frac{1}{2}\phi_u), \\ f_4^s(st) &= A_t \cos^2(\chi_t + \frac{1}{2}\phi_t) - A_u[\sin^2(\chi_u + \frac{1}{2}\phi_u) \\ &\quad + (\alpha_u z_u)^{-1}\sin^2\frac{1}{2}\phi_u], \\ f_5^s(st) &= -\frac{1}{2}A_t \sin(2\chi_t + \phi_t) + \frac{1}{2}A_u \sin(2\chi_u + \phi_u),\end{aligned}\quad (44)$$

where  $A_u$  is obtained from  $A_t$  by replacing  $t$  by  $u$  at the same  $s$ . Similar definitions apply to  $\chi_u$ ,  $\phi_u$ , and  $\alpha_u$ . The unpolarized differential cross section for one-pole

<sup>28</sup> Similar formulas, but without the  $u$ -channel contributions, have been given earlier by I. J. Muzinich, Phys. Rev. **130**, 1571 (1963); D. H. Sharp and W. G. Wagner, *ibid.* **131**, 2226 (1963).

dominance is given by

$$4\pi^2 s (d\sigma/d\Omega)_{\text{pole}} = |A_t|^2 + |A_u|^2 + \text{Re}(A_t^* A_u) [\cos(2\chi_t + 2\chi_u + \phi_t + \phi_u) - (\alpha_t z_t)^{-1} \sin^2 \frac{1}{2} \phi_t - (\alpha_u z_u)^{-1} \sin^2 \frac{1}{2} \phi_u] + O(z_i^{-2}). \quad (45)$$

This does not depend sensitively on the angle  $\phi_t$ , which depends on the relative coupling  $\beta_{11}/\beta_{00}$  in the  $t$  channel. In fact, (45) is more sensitive to the parameters contained in  $A_t$  than to  $\phi_t$ . We shall make the simplest choice<sup>29</sup>

$$\phi_t = 0, \quad (46)$$

or, equivalently,  $\beta_{11} = 0$ , which means that we neglect the coupling to the triplet spin state of  $p\bar{p}$  in the  $t$  channel. The hypothesis can be directly tested only by measuring the individual helicity amplitudes. It is very expedient for our purpose, for (44) becomes

$$f^s(s, t) = A_t \begin{pmatrix} \sin^2 \chi_t \\ -\cos^2 \chi_t \\ \sin^2 \chi_t \\ \cos^2 \chi_t \\ -\frac{1}{2} \sin 2\chi_t \end{pmatrix} + A_u \begin{pmatrix} \sin^2 \chi_u \\ -\cos^2 \chi_u \\ -\cos^2 \chi_u \\ -\sin^2 \chi_u \\ \frac{1}{2} \sin 2\chi_u \end{pmatrix}, \quad (47)$$

where the information about the specific trajectory used is contained solely in the functions  $A_t$  and  $A_u$ . In fact, the effect of  $n$  Regge trajectories can be taken into account by a redefinition

$$A_t = \sum_{i=1}^n A_{ti}, \quad (48)$$

where  $A_{ti}$  is the quantity corresponding to (43) for the  $i$ th trajectory. Substituting (47) into (5), we obtain

$$d\sigma/d\Omega = (4\pi^2 s)^{-1} [|A_t|^2 + |A_u|^2 + \text{Re}(A_t^* A_u) \cos(2\chi_t + 2\chi_u)] + O(z_i^{-2}), \quad (49)$$

which holds for any number of Regge trajectories, under the assumption (46) for each trajectory. We note in passing that

$$\chi_t + \chi_u = \chi_s, \quad \cos \chi_s = [tu/(t-4m^2)(u-4m^2)]^{1/2}.$$

## 5. REGGE CUTS

The presence of a Regge cut from  $J = -\infty$  to  $J = \alpha_c(t)$  in a signed partial-wave amplitude of given parity means that we can write

$$G_{\lambda\mu}(J, t) = 2\pi i \int_{-\infty}^{\alpha_c(t)} d\alpha \frac{\gamma_{\lambda\mu}(\alpha, t)}{J - \alpha} + S_{\lambda\mu}(J, t), \quad (50)$$

which is analogous to (32). Again, the part of  $S_{\lambda\mu}(J, t)$

<sup>29</sup> There is some evidence that  $\beta_{11}$  is small compared to  $\beta_{00}$ . First, phenomenological fits in the diffraction region have this property. Secondly, it is expected that  $\beta_{11} = 0$  at  $\alpha = 0$  [see Eq. (A8)], and if  $\beta_{11}$  were elsewhere large we would expect the cross section to have a dip at  $\alpha = 0$ , which according to our later choice of  $\alpha$  corresponds to  $-t = 2(\text{BeV}/c)^2$ . There is no dip in the data.

containing terms necessary for the Pauli principle can be effectively ignored.

If we regard a Regge cut as having its dynamical origin in the simultaneous exchange of more than one Regge pole, then in contradistinction to a Regge pole, we would generally expect the same Regge cut to appear in partial-wave amplitudes of both signatures and both parities.

The properties of  $\beta_{\lambda\mu}$  expressed by (34) are shared by  $\gamma_{\lambda\mu}$ , for they are general properties of partial-wave amplitudes. In particular, a factorization property analogous to (33) can be proved for  $\gamma_{\lambda\mu}$  by an analogous method based on two-body unitarity. In analogy with (34) and (46), we put

$$\gamma_{00}(\alpha, t) = (k_t^2/s_2)^{\alpha-1} D_0(\alpha, t), \quad \gamma_{10}(\alpha, t) = \gamma_{11}(\alpha, t) = 0, \quad (51)$$

where  $s_2$  is an arbitrary scale. Little is known about  $D_0(\alpha, t)$  except that it is real, and should vanish at the branch point  $\alpha = \alpha_c(t)$ .<sup>30</sup> If  $G_{\lambda\mu}(J, t)$  has parity  $(-)^J$  and signature  $\eta$ , then the Regge cut represented by the first term of (50), with the choice (51), gives the following contributions to  $g_i(s, t)$ :

$$g_1(s, t) = \int_{-\infty}^{\alpha_c(t)} \frac{d\alpha}{\sin \pi \alpha} \left( \frac{s-u}{2s_2} \right)^{\alpha-1} (e^{-i\pi\alpha} + \eta) \psi(\alpha, t) + O(z_i^{-2}),$$

$$g_2 = g_3 = g_4 = g_5 = 0, \quad (52)$$

where

$$\psi(\alpha, t) = \pi^{1/2} (\alpha + \frac{1}{2}) [\Gamma(\alpha + \frac{1}{2}) / \Gamma(\alpha + 1)] D_0(\alpha, t). \quad (53)$$

Asymptotically we expect

$$g_1(s, t) \xrightarrow{(s-u) \rightarrow \infty} (e^{-i\pi\alpha_c} + \eta) [(s-u)/2s_2]^{\alpha_c-1} \times \{ \ln[(s-u)/2s_2] \}^{-1-\epsilon} \zeta(t), \quad (54)$$

where  $\epsilon > 0$ , and  $\zeta(t)$  is some average of  $\psi(\alpha, t)/\sin \pi \alpha$  about  $\alpha = \alpha_c$ . An important simple feature of this formula is that, just as in the case of Regge pole, its phase is given by  $-\frac{1}{2}\pi\alpha_c$  for  $\eta = +1$ , and by  $-\frac{1}{2}\pi(\alpha_c - 1)$  for  $\eta = -1$ . However, evaluation of (52) with various simple forms of  $\psi(\alpha, t)$  indicates that the approach to the asymptotic phase is logarithmically slow. Typically, one finds an asymptotic criterion of the form

$$\ln[(s-u)/2s_2] \gg \pi. \quad (55)$$

As an estimate for orientation let us take  $s_2 = 1 \text{ BeV}^2$ . Then in order that  $\ln[(s-u)/2s_2] > 5\pi$ , say, we must have  $p_{\text{lab}} > 2700 \text{ BeV}/c$ . In energy ranges now available in the laboratory, therefore, the phase of (52) probably bears no simple relation to  $\alpha_c$  and  $\eta$ . For practical purposes we adopt the phenomenological form

$$g_1(s, t) = [(s-u)/2s_2]^{\alpha_c-1} e^{i(\omega - \pi\alpha_c/2)} R', \quad (56)$$

<sup>30</sup> V. N. Gribov, I. Ya. Pomeranchuk, and K. A. Ter-Martorossyan, Phys. Rev. **139**, B184 (1965); J. B. Bronzan and C. E. Jones *ibid.* **160**, 1494 (1967).

where  $\omega$  and  $R'$  are real functions of  $t$  and  $\ln s$ . We shall ignore the dependence on  $\ln s$ , for it changes little over the experimental range of  $s$ . The amplitude (56) contributes to the  $s$ -channel helicity amplitudes through an additive term  $A_t^c$  in the function  $A_t$  of (47), with

$$A_t^c = [(s-u)/2s_2]^{\alpha_c} \exp[i(\omega - \frac{1}{2}\pi\alpha_c)]R, \quad (57)$$

where  $\omega$  and  $R$  are in principle functions of  $t$  and  $\ln s$ , but in practice are taken to be functions only of  $t$ .

## 6. DETERMINATION OF EFFECTIVE TRAJECTORIES FROM EXPERIMENTS

We shall present experimental evidence that (a) at large  $-t$ , the  $p\bar{p}$  cross section is dominated by a single trajectory in some range of  $-t$ , and by another trajectory in an adjacent range of  $-t$ ; (b) the properties of the two trajectories are consistent, respectively, with those of the  $P$  trajectory and the  $P$ - $P$  cut generated by it.

Evidence for (a) is fairly direct. Evidence for (b), of course, makes use of theoretical ideas about the  $P$  trajectory. What we do is to compare the cross section (49) with experiments, using

$$A_t = \left(\frac{s-u}{2s_1}\right)^{\alpha(t)} \lambda(t), \quad (58)$$

where  $\lambda(t)$  is an arbitrary complex function. Since (43) and (57) both have this general form, we are testing the hypothesis that a single trajectory dominates, be it a pole or a cut.

We first note a prediction of (49) which depends mainly on the Pauli principle. Differentiating (49) with respect to  $\sin\theta$  at constant  $s$ , we obtain

$$\left[ \frac{\partial}{\partial \sin\theta} \left( \ln \frac{d\sigma}{d\Omega} \right) \right]_{\theta=90^\circ} = - \frac{8k^4}{1 + \frac{1}{2} \cos 4\chi} \left\{ \frac{A''}{A} + \left( \frac{A'}{A} \right)^2 + \frac{1}{2} \left[ \frac{A''}{A} - \left( \frac{A'}{A} \right)^2 \right] \cos 4\chi - 2\chi'' \sin 4\chi \right\}, \quad (59)$$

where  $\chi = \chi_t$ ,  $A = A_t$ , and a prime denotes differentiation with respect to  $t$  at fixed  $s$ . The right-hand side is to be evaluated at  $\theta = 90^\circ$ , where  $t = -2k^2$ . The notable property of (59) is that it is finite. This is mainly a consequence of the Pauli principle, which makes the cross section symmetric in  $u$  and  $t$ . The contribution to (59) from the  $t$  channel alone is proportional to  $\partial t / \partial(\sin\theta) = 2k^2 \tan\theta$ , which diverges at  $\theta = 90^\circ$ . However, the  $u$ -channel contribution, which is proportional to  $\partial u / \partial(\sin\theta) = -2k^2 \tan\theta$ , cancels the divergence and makes the result finite. In elastic scattering of non-identical particles such as  $p\bar{p}$  and  $\pi p$ , we expect the quantity corresponding to (59) to be infinite. It would be interesting to test this experimentally. The finiteness

of (59) is strikingly demonstrated in the experiment of Ref. 7. Its  $s$  dependence involves a more detailed knowledge of  $A_t$ , and is not our concern in this section (see Sec. 7 and Fig. 4), but it is expected to be a rapidly decreasing function of  $s$ .

To turn to our main task, we find it convenient to regard the cross section as a function of  $t$  and  $\theta$ , instead of the more usual variables  $t$  and  $s$ . This means that  $s$  and  $u$  take the forms

$$\begin{aligned} s &= 4(k^2 + m^2) = 4m^2 - 2t(1 - \cos\theta)^{-1}, \\ u &= t \cot^2 \frac{1}{2}\theta. \end{aligned} \quad (60)$$

We also write

$$\begin{aligned} A_t &\equiv A(t, \theta) = \lambda(t) \left[ \frac{1}{2s_1} \left( 4m^2 - \frac{t(3 + \cos\theta)}{1 - \cos\theta} \right) \right]^{\alpha(t)}, \\ A_u &\equiv \bar{A}(t, \theta) = \lambda(u) \left[ \frac{1}{2s_1} \left( 4m^2 - \frac{t(3 - \cos\theta)}{1 - \cos\theta} \right) \right]^{\alpha(u)}, \\ \chi_t &\equiv \chi(t, \theta) = \cos^{-1} \left( \frac{2m^2(1 - \cos\theta) - t}{t - 4m^2} \right)^{1/2}, \\ \chi_u &\equiv \bar{\chi}(t, \theta) = \cos^{-1} \left( \frac{2m^2(1 - \cos\theta) - t}{t - 4m^2 \tan^2 \frac{1}{2}\theta} \right)^{1/2}. \end{aligned} \quad (61)$$

At given  $t$  and  $\theta = 90^\circ$  the differential cross section is given by

$$\begin{aligned} (d\sigma/d\Omega)_{t, 90^\circ} &= [4\pi^2(2m^2 - t)]^{-1} |A(t, 90^\circ)|^2 \\ &\quad \times (1 + \frac{1}{2} \cos 4\chi), \quad (62) \\ \chi &\equiv \chi(t, 90^\circ). \end{aligned}$$

As  $\theta$  is decreased from  $90^\circ$  at fixed  $t$ , the  $u$ -channel contribution  $A_u$  becomes increasingly small, provided that  $\alpha(u) < 0$ . The rapidity of the decrease depends on  $\alpha(u)$  and on the scale  $s_1$ , which cannot be determined *a priori*. For the present we shall make the rough guess, to be justified by the consistency of the results, that  $A_u$  can be neglected to 10% accuracy for  $\theta < 80^\circ$ . We then have

$$(d\sigma/d\Omega)_{t, \theta < 80^\circ} \approx \{8\pi^2[2m^2 - t(1 - \cos\theta)^{-1}]\}^{-1} \times |A(t, \theta)|^2. \quad (63)$$

Let us put

$$I(t, \theta) \equiv (d\sigma/d\Omega)_{t, \theta} / (d\sigma/d\Omega)_{t, 90^\circ}. \quad (64)$$

Dividing (63) by (62), and using (61), we obtain

$$\begin{aligned} I(t, \theta < 80^\circ) &\simeq \left( \frac{4m^2 - t(3 + \cos\theta)(1 - \cos\theta)^{-1}}{4m^2 - 3t} \right)^{2\alpha(t)} (m^2 - \frac{1}{2}t) \\ &\quad \times (1 + \frac{1}{2} \cos 4\chi)^{-1} [2m^2 - t(1 - \cos\theta)^{-1}]^{-1}. \end{aligned} \quad (65)$$

The important thing about this expression is that the arbitrary function  $\lambda(t)$  no longer appears. Solving for

$\alpha(t)$  we obtain

$$\alpha(t) \approx \frac{\ln\{I(t,\theta)(1+\frac{1}{2}\cos 4\chi)[2m^2-t(1-\cos\theta)^{-1}](m^2-\frac{1}{2}t)^{-1}\}}{2\ln\{[4m^2-t(3+\cos\theta)(1-\cos\theta)^{-1}](4m^2-3t)^{-1}\}}, \quad (66)$$

where  $\chi$  is defined in (62), and  $I(t,\theta)$  is to be calculated from experimental data. This formula is approximately valid only for  $\theta < 80^\circ$ , when the right-hand side is supposed to be independent of  $\theta$ .

The approximations involved in (66) are the following. First, we have neglected  $O(z_i^{-2})$  in  $d\sigma/d\Omega$ . Secondly, as indicated by (46), we have neglected the coupling of the trajectory to the triplet spin state of  $p\bar{p}$  in the  $t$  channel. Finally, we have neglected  $A_u$  in (63). Unfortunately these approximations are unavoidable, for we would not have been able to extract  $\alpha(t)$  purely from the data without them. It means, however, that the expression (65) has a theoretical uncertainty in addition to experimental errors. As a guess, we assign to  $I(t,\theta)$  a theoretical uncertainty of 10%.

To calculate  $I(t,\theta)$ , we use the data in Refs. 5-7 for  $-t > 2.5$  (BeV/c)<sup>2</sup> and for  $57^\circ < \theta < 78^\circ$  to evaluate the numerator of (66). The denominator at the same  $t$  is taken from the data of Refs. 4 and 7, either directly or by interpolation. Experimental errors range from 3 to 10%. The result for  $\alpha(t)$  calculated in the manner described is shown in Fig. 1.

It is consistent with the data to suggest that a single trajectory  $\alpha_1(t)$  dominates the range  $3 < -t < 5$  (BeV/c)<sup>2</sup>,

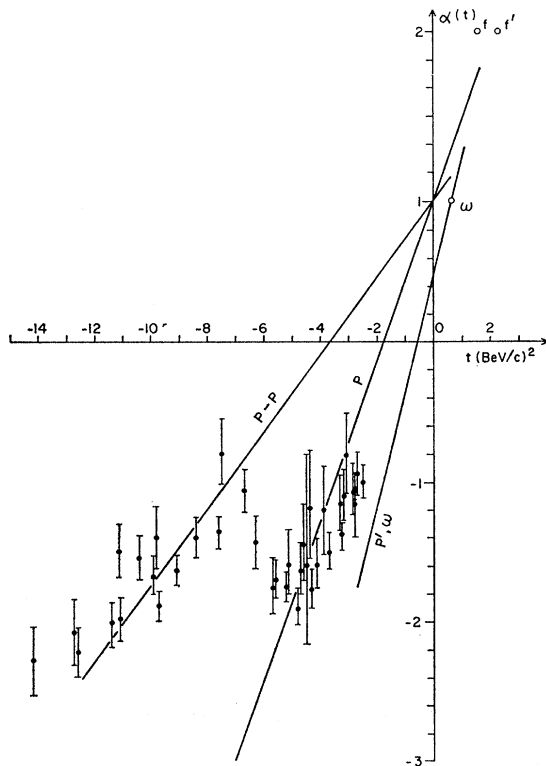


FIG. 1. The effective trajectory  $\alpha(t)$  for large-angle  $p\bar{p}$  scattering.

and another trajectory  $\alpha_2(t)$  dominates the range  $7 < -t < 13$  (BeV/c)<sup>2</sup>, with

$$\begin{aligned} \alpha_i(t) &= 1 + \alpha_i' t, & (i=1, 2) \\ \alpha_1' &= 0.55 \pm 0.05 \quad (\text{BeV/c})^{-2}, & (67) \\ \alpha_2' &\approx \frac{1}{2} \alpha_1'. \end{aligned}$$

In the region  $5 < -t < 7$  (BeV/c)<sup>2</sup>, both  $\alpha_1$  and  $\alpha_2$  are important, as evidenced by the fact that the effective trajectory lies between  $\alpha_1$  and  $\alpha_2$ . At  $t = -7$  (BeV/c)<sup>2</sup>, where  $\alpha_1 = -3$ ,  $\alpha_2$  takes over completely. The sharpness of the transition from  $\alpha_1$  to  $\alpha_2$  indicates that the contribution of  $\alpha_1$  tends to zero at  $\alpha = -3$ . This suggests that  $\alpha_1$  has positive signature, for in that case  $\alpha_1 = -3$  would be a nonsense wrong-signature point, where the contribution of  $\alpha_1$  should vanish in the absence of a fixed pole. On the other hand, at the nonsense wrong-signature point  $\alpha_1 = -1$  there must be a fixed pole, for otherwise the contribution of the trajectory  $\alpha_1$  would vanish, and the effective trajectory should switch to a different trajectory at that point. It is therefore consistent with the data to suggest that  $\alpha_1$  is a trajectory whose intercept at  $t=0$  is consistent with 1, and whose signature is positive. It seems irresistible to identify  $\alpha_1$  with the  $P$  trajectory.

Further support for the identification comes from the behavior of  $\alpha_2$ . If  $\alpha_1$  is the  $P$  trajectory, then exchanging two  $P$  trajectories in the  $t$  channel theoretically gives rise to the  $P$ - $P$  cut,<sup>3</sup> whose branch point should have the trajectory

$$\alpha_c(t) = 2\alpha_1(t/4) - 1. \quad (68)$$

Using the linear form (67) for  $\alpha_1$ , we obtain

$$\alpha_c(t) = 1 + \frac{1}{2} \alpha_1' t, \quad (69)$$

which is consistent with the identification  $\alpha_2 = \alpha_c$ .

The exchange of  $n$   $P$  trajectories in the  $t$  channel should lead to a Regge cut with branch point trajectory given by<sup>3</sup>

$$\alpha_n(t) = n\alpha_1(t/n^2) - n + 1. \quad (70)$$

which for linear  $\alpha_1$  becomes

$$\alpha_n(t) = 1 + \alpha_1' t/n. \quad (71)$$

Since they have successively smaller slopes, those with  $n > 2$  may dominate over  $\alpha_2$  as  $-t$  increases. The tendency for  $\alpha$  in Fig. 1 to deviate upwards away from  $\alpha_2$  at  $-t > 12$  (BeV/c)<sup>2</sup> may be attributed to the increasing importance of  $\alpha_n$  for  $n \geq 3$ . On the other hand, the fact that  $\alpha_2$  takes over from  $\alpha_1$  only when  $-t$  is sufficiently large, and that  $\alpha_{n \geq 2}$  begins to take over only when  $-t$  is still larger, suggests that the effective coupling of  $\alpha_{n \geq 2}$  is much smaller than that of  $\alpha_2$ , and

that the effective coupling of  $\alpha_2$  is much smaller than that of  $\alpha_1$ .

For  $-t < 3$  (BeV/c)<sup>2</sup> there is a distinct tendency for  $\alpha$  in Fig. 1 to deviate from  $\alpha_1$  towards the known trajectories of  $\omega$  and  $P'$ . This is consistent with our knowledge that the latter gives important contribution in the diffraction region.

The type of fixed poles and Regge cuts considered here have a common dynamical origin, i.e., the third double spectral function of Mandelstam.<sup>3,12</sup> Thus one expects that fixed poles and cuts generally go hand in hand. The fact that our interpretation of  $\alpha_1$  as the  $P$  trajectory simultaneously calls for a fixed pole at  $\alpha_1 = -1$ , and the identification of  $\alpha_2$  as the  $P$ - $P$  cut is in conformity with this expectation.

While the foregoing interpretation is consistent with the data, it is of course not required by them. For example, an alternative interpretation may be that  $\alpha_2$  is the  $P$  trajectory. This would make  $\alpha_1$  a new trajectory so far undiscovered, for all known trajectories other than the  $P$  trajectory have steeper slopes. The relation  $\alpha_2' \approx \frac{1}{2}\alpha_1'$  would then appear to be an accident. Hence it should be emphasized that our interpretation is motivated mainly by the fact that with it, all salient features of the data seem to fall into place naturally, and conversely all salient features of the theoretical model seem to find reflections in the data.

Assuming the correctness of our identifications, we summarize the findings as follows:

(a) The  $P$  trajectory  $\alpha_1$  is consistent with a straight line of slope 0.5 (BeV/c)<sup>2</sup>. A linear extrapolation of the trajectory passes through  $\alpha = 2$  near the masses of the  $f_0$  and  $f_0'$  mesons.<sup>31</sup>

(b) The  $P$ - $P$  cut trajectory has half the slope, and it has a much smaller effective coupling than  $P$ . There is a hint of the  $P$ - $P$ - $P$  and higher cuts, whose effective couplings would be smaller still.

(c) There is a fixed pole at the first nonsense wrong-signature point  $\alpha_1 = -1$ , but there is no fixed pole at the second nonsense wrong-signature point  $\alpha_1 = -3$ .

Thus the most remarkable feature of the cross section, namely, the break first observed at  $\theta = 90^\circ$  in the Argonne experiment,<sup>4</sup> is attributed to the fact that at that point  $P$  passes through the nonsense wrong-signature value  $\alpha_1 = -3$ . Similar phenomena associated with nonsense wrong-signatures points of various trajectories have been observed before in  $\pi\bar{p}$  charge-exchange scattering ( $\rho$  trajectory),<sup>32</sup>  $\pi\bar{p}$  backward scattering (nucleon trajectory),<sup>33</sup> and  $\pi^0$  photoproduction ( $\omega$  trajectory).<sup>34</sup> In all these cases, however, dips in the cross sections occur at the first nonsense wrong-signature point, whereas in our case the dip (modified

by cut contributions) occurs at the second nonsense wrong-signature point. Why this is so seems to be entirely a dynamical question, which we shall not discuss here.

The considerations here have the virtue that they are independent of detailed assumptions concerning pole residues and cut discontinuities. However, they involve approximations that cannot be improved without destroying the very purpose they serve. It is therefore important that we try to fit the cross section in detail, for failure to fit will disprove the interpretation.

## 7. A MODEL

### A. Cross Section

We make use of the ideas expressed in Sec. 6 to fit the  $p\bar{p}$  cross section in the region

$$\begin{aligned} 5 < p_{\text{lab}} < 26 \quad \text{BeV}/c, \\ 3 < -t < 18 \quad (\text{BeV}/c)^2, \end{aligned} \quad (72)$$

where the effects of the  $P'$  and  $\omega$  trajectories are assumed to be negligible. A model is set up using the  $P$  trajectory plus the first two Regge cuts generated by it, with the  $P$  trajectory taken to be

$$\begin{aligned} \alpha_1(t) &\equiv \alpha_{1t} = 1 + \alpha't, \\ \alpha' &= 0.55 \quad (\text{BeV}/c)^{-2}. \end{aligned} \quad (73)$$

The two cuts included are the  $P$ - $P$  and  $P$ - $P$ - $P$  cuts, whose branch points have respective trajectories

$$\begin{aligned} \alpha_2(t) &\equiv \alpha_{2t} = 1 + \frac{1}{2}\alpha't, \\ \alpha_3(t) &\equiv \alpha_{3t} = 1 + \frac{1}{3}\alpha't. \end{aligned} \quad (74)$$

The  $s$ -channel helicity amplitudes are given by (47), with

$$\begin{aligned} A_t &= A_1(s,t) + A_2(s,t) + A_3(s,t), \\ A_u &= A_1(s,u) + A_2(s,u) + A_3(s,u), \end{aligned} \quad (75)$$

where

$$\begin{aligned} A_1(s,t) &= K_1 \exp\left(\frac{1}{2}i\pi\alpha_{1t}\right) \Gamma(1-\alpha_{1t}) (1+\alpha_{1t})^{-1} \\ &\quad \times \sin\left[\frac{1}{2}\pi(1+\alpha_{1t})\right] [(s-u)/2s_1]^{\alpha_{1t}}, \\ A_2(s,t) &= K_2 c_2 \exp\left[i\left(\omega_2 + \frac{1}{2}\pi\alpha_{2t}\right)\right] [(s-u)/2s_2]^{\alpha_{2t}}, \\ A_3(s,t) &= K_3 c_3 \exp\left[i\left(\omega_3 + \frac{1}{2}\pi\alpha_{3t}\right)\right] [(s-u)/2s_3]^{\alpha_{3t}}, \end{aligned} \quad (76)$$

where

$$\begin{aligned} c_2 &= (t\alpha_{2t}/m)^2, \\ c_3 &= (t/m)^2, \end{aligned} \quad (77)$$

and  $K_i$ ,  $\omega_i$ , and  $s_i$  are real constants, with  $K_i > 0$ ,  $s_i > 0$ . The choice for  $A_1$  corresponds to (42) with  $\eta = 1$ ,  $\lambda_1 = 0$ , and

$$\lambda_0(t) = 2\pi^{-1/2} K_1 (m^2 - \frac{1}{4}t) [(1+\alpha_t)\Gamma(\alpha_t + \frac{3}{2})]^{-1}, \quad (78)$$

where a fixed pole at  $\alpha_t = -1$  is assumed, as suggested in Sec. 6. The factor  $m^2 - \frac{1}{4}t$  is thrown in for no reason other than to make the final formulas simple. The factor  $[\Gamma(\alpha_t + \frac{3}{2})]^{-1}$  is explained in the Appendix

<sup>31</sup> A linear trajectory passing through  $f_0'$  would have  $\alpha' = 0.435$ . For  $f_0$  it would be  $\alpha' = 0.64$ .

<sup>32</sup> F. Arbab and C. B. Chiu, Phys. Rev. **147**, 1045 (1966).

<sup>33</sup> C. B. Chiu and J. Stack, Phys. Rev. **153**, 1575 (1967).

<sup>34</sup> M. P. Locher and H. Rollnick, Phys. Letters **22**, 696 (1966).

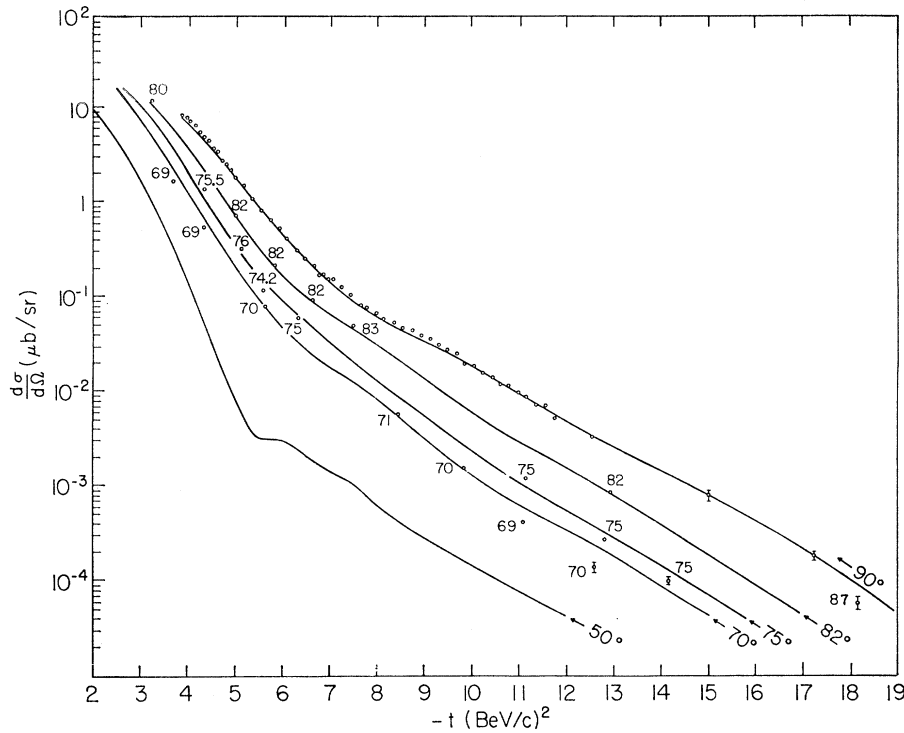


FIG. 2. The  $pp$  differential cross section as a function of invariant momentum transfer squared  $-t$  at fixed c.m. scattering angle  $\theta$ . Solid curves are theoretical fits. Numbers attached to data points correspond to  $\theta$ . Statistical errors, wherever not shown, are equal to or smaller than the size of the points. The data are taken from Refs. 4-7, but not all data points are shown.

[see Eq. (A6)]. The forms of  $A_2$  and  $A_3$  correspond to (57), with  $R$  taken to be, respectively, proportional to  $(\alpha_c t)^2$  and  $t$  for the two cuts, and  $\omega_i = \text{const}$ . We have no reason for these choices apart from the fact that

they give a good fit to experiments. Other variations considered are listed in Table III. The cross section is given by (49), which will contain eight real adjustable parameters:  $K_1, K_2, K_3, s_1, s_2, s_3, \omega_2,$  and  $\omega_3$ .

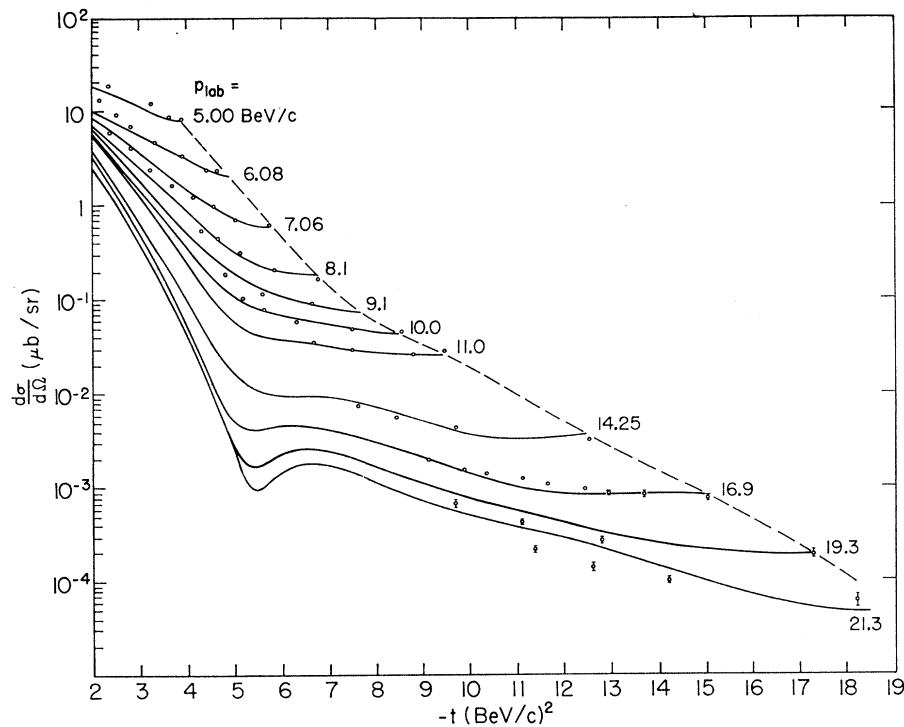


FIG. 3. The  $pp$  differential cross section as a function of invariant momentum transfer squared  $-t$  at fixed incident laboratory momentum  $p_{\text{lab}}$ . Data points at  $\theta=90^\circ$ , shown in Fig. 2, are omitted here. Solid lines represent theoretical fits. Data points used in the fit are a subset of the data points shown here plus the points at  $\theta=90^\circ$ . Sources of data are Refs. 4-7.

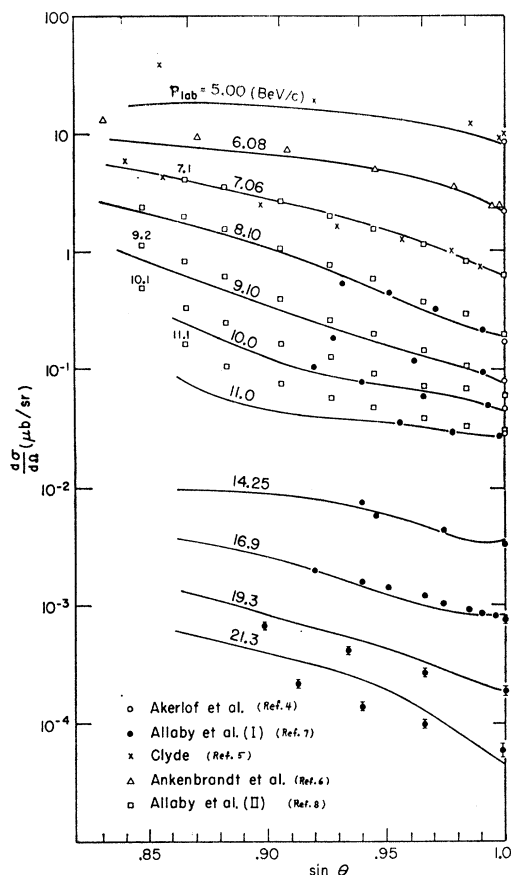


FIG. 4. The  $pp$  differential cross section as a function of  $\sin\theta$ , where  $\theta$  is the c.m. scattering angle, at fixed incident laboratory momentum  $p_{\text{lab}}$ . The finiteness of the slopes of the curves at  $\sin\theta=1$  is a consequence of the Pauli principle. If there were no Pauli principle, the slopes would have been infinite. Solid curves are theoretical fits. Except for the open squares,  $p_{\text{lab}}$  for the data points are the same as those labeled on the nearest theoretical curve. The open squares are new data available after the fits were made. It is apparent by inspection that they differ significantly in absolute normalization from older data from the same laboratory (solid circles).

It was noted in Sec. 5 that a Regge cut is generally expected to be coupled to partial-wave amplitudes of both signatures and parities. Signature, however, becomes lost when we use the phenomenological forms in (63), for in those forms the signature can enter only through  $\omega_1$  and  $\omega_2$ , which are adjustable parameters. We specifically neglect partial-wave amplitudes of parity  $(-)^J$  for simplicity.

TABLE III. Various choices for  $c_2$  and  $c_3$  [see Eq. (77)].

$c_2$	$c_3$	Ave. $\chi^2/\text{point}$
$(i\alpha_{2t}/m)^2$	$t/m$	6.6
$(i\alpha_{2t}/m)^2$	$i\alpha_{3t}/m$	9.2
$(\alpha_{2t}/m)^2$	$(i\alpha_{3t}/m)^2$	9.7
$(\alpha_{2t}/m)^2$	$(\alpha_{3t}/m)^2$	11.0
1	1	19.0

A total of 97 data points, selected for their small statistical errors, are used in a least-squares fit to determine the eight parameters.<sup>35</sup> The best fit has an average  $\chi^2$  of 6.6 per datum point,<sup>36</sup> and corresponds to

$$\begin{aligned} K_1 &= 0.20, & \sqrt{s_1} &= 1.75 \text{ BeV}, \\ K_2 &= 0.0057, & \sqrt{s_2} &= 0.925 \text{ BeV}, & \omega_2 &= -2.89, \\ K_3 &= 0.0011, & \sqrt{s_3} &= 2.50 \text{ BeV}, & \omega_3 &= -0.354. \end{aligned} \quad (79)$$

We have tried replacing  $c_2$  and  $c_3$  in (77) by other choices. For the record they are listed in Table III

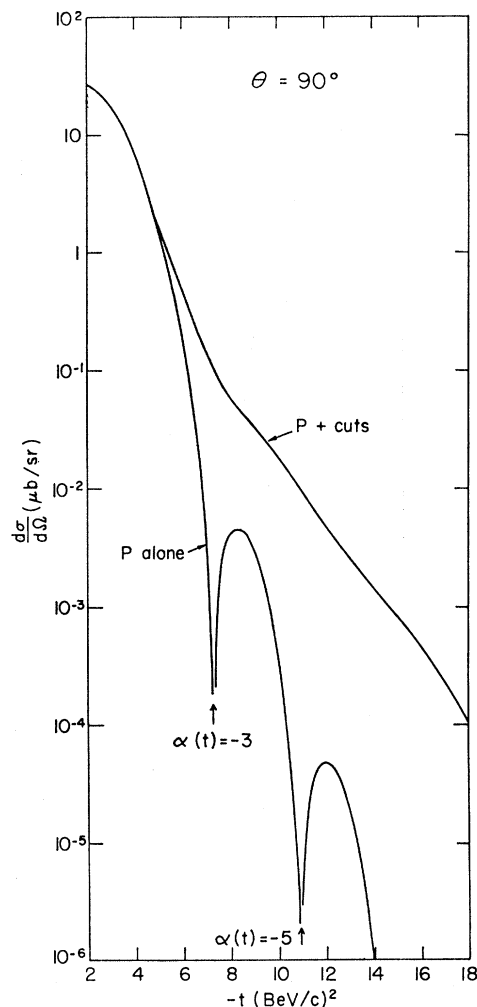


FIG. 5. The upper curve represents the theoretical fit to the differential cross section at  $\theta=90^\circ$ . The lower curve is obtained by omitting contributions of the Regge cuts in the theoretical formula. The break at  $-t=7$  ( $\text{BeV}/c$ )<sup>2</sup> is caused by the fact that the  $P$  trajectory passes through the nonsense wrong-signature value  $\alpha = -3$  at that point. At  $\alpha = -1$  a fixed pole is assumed to be present.

<sup>35</sup> We thank Dr. W. Rarita for making available to us the computer program VARMIT, with which the fit was carried out.

<sup>36</sup> The  $\chi^2$  takes into account only statistical errors in the experiments, and not systematic errors. Thus the  $\chi^2$  value is not meaningful as an indication of how well the model agrees with experiments.

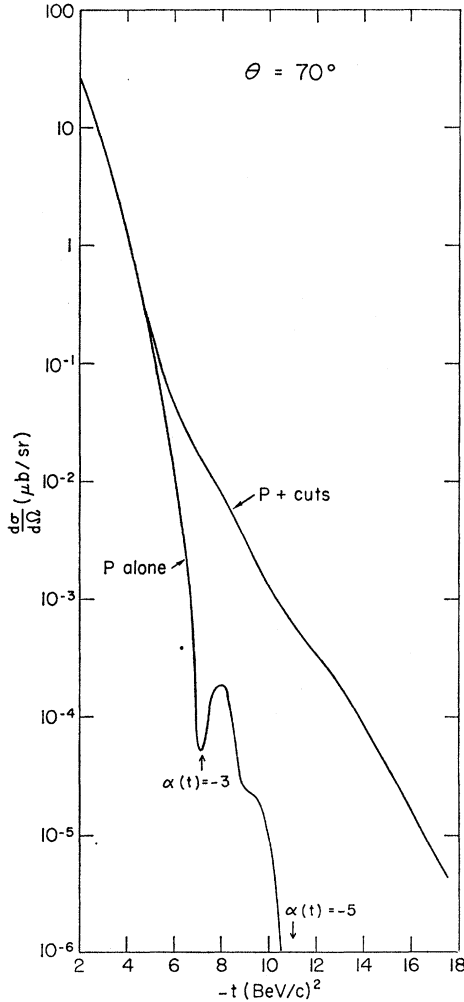


FIG. 6. Same as Fig. 5 except for  $\theta=70^\circ$ . The break shifts to  $-t \approx 6$  (BeV/c) $^2$ , because of  $u$ -channel contributions.

with the  $\chi^2$  of the fits. The case (77) is the one with the least  $\chi^2$ . We note, however, that while a majority of the data points used in the fit have statistical errors of  $\sim 3\%$  the theoretical formulas cannot be trusted to better than  $10\%$ , even if the model is basically valid. Hence it is not meaningful to distinguish between values of  $\chi^2$  below  $\sim 10$ .

A comparison between theory and experiment is shown in Figs. 2-4 in various methods of plotting. More data are plotted than the 97 points used in the fitting. In Figs. 5 and 6 are shown the contribution from the  $P$  trajectory alone as compared with the total contribution from  $P$ +cuts, for  $\theta=90^\circ$ ,  $70^\circ$ . It is seen that for  $-t < 5$  (BeV/c) $^2$  the cuts can be neglected, and for  $t > 6$  (BeV/c) $^2$  the pole can be neglected.

It is evident in Figs. 5 and 6 that for different  $\theta$  the sharp break in the differential cross section does not occur at the same value of  $-t$ . As  $\theta$  decreases from  $90^\circ$ , the break shifts towards a smaller value of  $-t$ . This may seem puzzling at first sight, in view of the fact

that in our model the break is associated with  $\alpha_1(t) = -3$ . The cause of the shift, of course, is the  $u$ -channel contribution. At  $\theta=90^\circ$ , we have  $t=u$  and at the break  $\alpha_1(t) = \alpha_1(u) = -3$ ; but at  $\theta=70^\circ$ ,  $\alpha_1(u) \neq -3$  at the break.

After we had completed our fit, some 86 additional data points became available from the CERN group,<sup>8</sup> some of which are plotted as open squares in Fig. 4. It is seen that they follow the shape of the theoretical curves, but do not agree in normalization. The reason is that they differ significantly in absolute normalization from earlier data by the same group, indicated by solid circles. Although we understand that the absolute normalization of the new data is more reliable, we have not readjusted our fit to the new data.

The fit to the cross section shows that there is so far no inconsistency between experiments and our hypotheses regarding the  $P$  trajectory and associated cuts.

### B. Polarization

The polarization parameter  $\mathcal{P}$  is defined by

$$\mathcal{P} = 2 \operatorname{Im}[(f_1^s + f_2^s + f_3^s - f_4^s)f_5^{s*}] / \sum_{i=1}^5 |f_i^s|^2. \quad (80)$$

The amplitude  $f_5^s$  vanishes at  $\theta=0$  because of angular-momentum conservation [see (21)], and vanishes at  $\theta=90^\circ$  because of the Pauli principle [see (6)]. The polarization must therefore vanish at  $\theta=0$  and at  $\theta=90^\circ$ . This should be true regardless of the model in which  $\mathcal{P}$  is calculated.

For single Regge-pole exchange,  $\mathcal{P} \approx 0$  in the diffraction region  $\theta \rightarrow 0$ , because in that region the  $u$ -channel Regge pole can be neglected, and the  $t$ -channel Regge

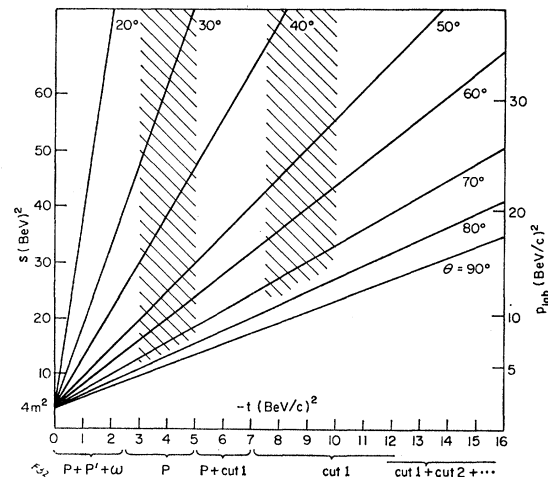


FIG. 7. Dominating trajectories for various ranges of  $-t$  are indicated below the abscissa. Shaded areas correspond to kinematic regions in which  $pp$  scattering is dominated by a single trajectory, and in which the  $u$ -channel contribution is negligible. Hence they are regions in which the polarization should be small. Because of the Pauli principle, the polarization must vanish along the line  $\theta=90^\circ$ .

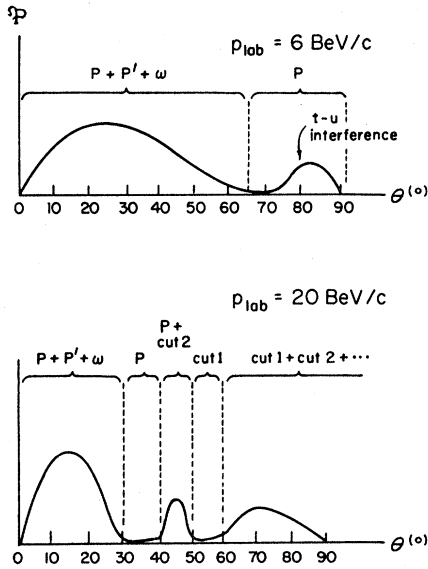


FIG. 8. Qualitative predictions for the behavior of the polarization in  $pp$  scattering. The relative signs of the polarization in different regions are uncertain. Dominating trajectories for various ranges are indicated.

pole contributes the same phase to all  $f_i^s$ . Any observed polarization in the diffraction region must therefore be attributed to the existence of more than one Regge pole, presumably  $P$ ,  $P'$ , and  $\omega$ . We are, however, not concerned here with the diffraction region.

According to our model, the  $P$  trajectory alone is dominant in the region  $3 < t < 5$  ( $\text{BeV}/c$ )<sup>2</sup>. Therefore, in that region we expect  $\mathcal{P} \approx 0$  for  $\theta \ll 90^\circ$ , where the  $u$ -channel contribution can be neglected. As  $\theta$  increases towards  $90^\circ$ , the  $u$  channel becomes important, and its interference with the  $t$  channel would produce polarization. However,  $\mathcal{P} = 0$  at  $\theta = 90^\circ$ , as noted previously. Hence, we expect that  $\mathcal{P}$  passes through a maximum (or minimum) before  $\theta = 90^\circ$ , in the region of  $t$  considered. In the region where the  $P$ - $P$  cut alone dominates, a similar phenomenon occurs, but in other regions where more than one trajectory contributes there would always be polarization.

The regions in which the polarization is expected to be vanishingly small, according to our model, are the shaded regions in Fig. 6. For illustration, suppose  $\mathcal{P}$  is measured as a function of  $\theta$  at  $p_{\text{lab}} = 6$   $\text{BeV}/c$ . Then according to Fig. 6, we expect  $P$  to be dominant in the region  $65^\circ < \theta < 90^\circ$ , and the measurement might look qualitatively like the plot given in Fig. 7. Our expectation for  $p_{\text{lab}} = 20$   $\text{BeV}/c$  is shown in Fig. 8.

A measurement of  $\mathcal{P}$  near  $\theta = 90^\circ$  for  $p_{\text{lab}} \sim 6$   $\text{BeV}/c$  would give further information about the  $P$  trajectory,<sup>37</sup>

<sup>37</sup> Polarization at large angles have been measured below  $p_{\text{lab}} = 2.5$   $\text{BeV}/c$  by M. J. Longo, H. A. Neal, and O. E. Overseth, Phys. Rev. Letters **16**, 536 (1966); and H. A. Neal and M. J. Longo, Phys. Rev. **161**, 1374 (1967). However the energy is too low for our model to apply, for at their energies the effects of  $P'$  and  $\omega$  are important for the whole angular range.

for we can neglect all but the  $P$  trajectory:

$$4\pi^2 s (d\sigma/d\Omega) \mathcal{P} = \text{Im}(A_t^* A_u) \sin(2\chi_t + 2\chi_u + \phi_t + \phi_u), \quad (81)$$

where  $A_t$  is given by (43) with  $\eta = 1$ , and where the approximation (46) has not been made.

We shall not write out a general expression for  $\mathcal{P}$ , taking into consideration the  $P$  trajectory plus cuts, and keeping both singlet and triplet spin states in the  $t$  channel. With neglect of the triplet state,  $\mathcal{P}$  is still given by (81) with  $\phi_t = \phi_u = 0$ , and with  $A_t$  given by (48).

### C. Proton-Antiproton Scattering

The relation between  $p\bar{p}$  scattering and  $pp$  scattering has been discussed at the end of Sec. 2. We neglect the  $u$  channel entirely. If a single trajectory dominates in the  $t$  channel, then the  $t$ -channel amplitudes are given by (41), which leads to the differential cross section

$$d\sigma/d\Omega = (4\pi^2 s)^{-1} |A_t|^2 + O(z_t^{-2}), \quad (82)$$

where  $A_t$  is given by (43), and no special assumption has been made about  $\phi_t$ . At a sufficiently high energy this should be valid in the interval  $3 < -t < 5$  ( $\text{BeV}/c$ )<sup>2</sup>, where according to our model  $P$  dominates.

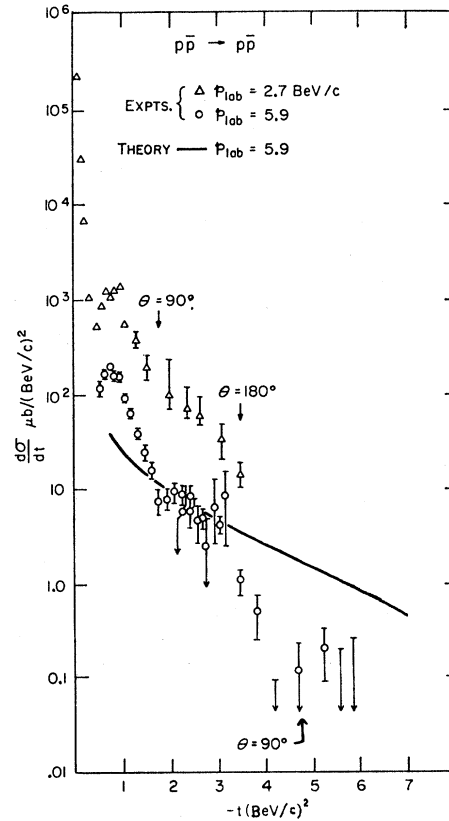


FIG. 9. Elastic  $p\bar{p}$  scattering. The data are taken from Refs. 19 and 38. The solid curve is an absolute calculation at  $p_{\text{lab}} = 5.9$   $\text{BeV}/c$  assuming  $P$ -trajectory exchange only, with parameters taken from our fit to  $pp$  scattering.

The only available experimental data that cover a wide angular range are measurements made at  $p_{\text{lab}} = 2.7$  BeV/c<sup>38</sup> and  $p_{\text{lab}} = 5.9$  BeV/c.<sup>19</sup> Although our model is not expected to be good at these low energies, it may still be interesting to compare the data with (82), in which  $A_t$  is calculated with the parameters of  $P$  determined from our  $p\bar{p}$  fit. The cuts are unimportant. The result of this absolute calculation of the  $p\bar{p}$  cross section at 5.9 BeV/c is shown in Fig. 9.

We note that the bumps in the cross section are not reproduced. They are presumably due to interference from the  $P'$  and  $\omega$  trajectories, which have been left out. In the interval  $3 < -t < 5$  (BeV/c)<sup>2</sup> the theoretical curve seems too high by a factor of 2-3, although the statistics are very poor there. If the discrepancy is real, it would indicate that the contribution of a nucleon-nucleon cut in the  $u$  channel may not be negligible.

### 8. SPECULATIONS ON PHENOMENA AT EXTREMELY HIGH ENERGIES

We make some projections into the extremely high energy domain, say, for  $p_{\text{lab}} > 200$  BeV/c. On the basis of our model, we expect the following phenomena to occur:

(a) At a given  $s$ , the effects of cuts are still negligible in a small neighborhood of  $t=0$ , in which the diffraction peak becomes dominated by  $P$  alone. This neighborhood, however, shrinks to zero as  $s \rightarrow \infty$ . Outside of this neighborhood, cuts become dominant and give  $d\sigma/d\Omega$  a smaller slope with respect to  $t$ . At any given  $t$  in the cut-dominant region, when  $s$  is sufficiently large, many cuts will contribute simultaneously, so that the slope of  $d\sigma/d\Omega$  is not simply related to the parameter of any single cut.

(b) In the cut-dominant region we can describe the qualitative behavior of the scattering amplitude  $f$  by neglecting spin and by taking into account only the cuts generated by  $P$ :

$$f = C \sum_{n=2}^{\infty} \gamma^n \left( \frac{s}{s_0} \right)^{1+\alpha' t/n}, \quad (83)$$

where  $\alpha'$  is the slope of the  $P$  trajectory. We have assumed the simple form  $\gamma^n$  for the coupling of the  $n$ th cut, where  $\gamma$  may be a function of  $\ln s$ . The  $u$  channel is neglected for simplicity. As  $s \rightarrow \infty$  at fixed  $t$ , the sum can be evaluated approximately by replacing it by an integral over  $n$ , and by calculating the integral by the method of saddle-point integration:

$$f \xrightarrow{s \rightarrow \infty} (\pi^{1/2} \alpha' C s \ln s) (-\lambda t)^{1/4} \exp[-2(-\lambda t)^{1/2}], \quad (84)$$

$$\lambda = -\alpha' (\ln s) (\ln \gamma).$$

Thus the exponential decrease with  $-t$ , which is characteristic of a single trajectory, is changed to

<sup>38</sup> V. Domingo, G. P. Fisher, L. Marshall Libby, and R. Sears, Phys. Letters, **24B**, 642 (1967).

exponential decrease with  $(-t)^{1/2}$ , which is the most rapid decrease allowed by analyticity.<sup>39</sup> The amplitude (84) leads to an expression for  $d\sigma/dt$  which depends on  $s$  only logarithmically, if  $C$  and  $\gamma$  are constants. An energy-independent limiting function<sup>40</sup> of  $t$  results if  $C \propto (\ln s)^{-1}$  and  $\gamma \propto \exp(\ln s)^{-1}$ .

### APPENDIX: COMPENSATION

The symmetry properties (30) and (31) imply that

(a) If at  $t=t_0$  a Regge trajectory passes through  $\alpha(t_0) = \text{half-integer}$  except  $-\frac{1}{2}$ , with residue  $\beta_{\lambda\mu}(t_0)$  in  $G_{\lambda\mu}(J, t)$ , then either  $\beta_{\lambda\mu}(t_0) = 0$ , or another trajectory of the same parity and signature must pass through  $-\alpha(t_0) - 1$ , with the same residue in  $G_{\lambda\mu}(J, t)$ .

(b) If at  $t=t_0$  a Regge trajectory passes through  $\alpha(t_0) = 0$  or  $-1$ , with residue  $\beta_{11}(t_0)$  in  $G_{11}(J, t)$ , then either  $\beta_{11}(t_0) = 0$ , or another trajectory of opposite parity and opposite signature must pass through  $-\alpha(t_0) - 1$ , with the same residue in the amplitude of opposite parity and signature to  $G_{11}(J, t)$ . The additional trajectories called for by (a) or (b) above will be referred to as compensating trajectories of type (a) or (b), respectively. They cancel unphysical singularities which would otherwise be present in the scattering amplitude. To see this we have to examine more closely the properties of  $E_{\lambda\mu}^{\alpha\pm}(z)$ .

We have the explicit representations

$$E_{00}^{\alpha+}(z) = \mathcal{P}_{\alpha}(z) = z^{\alpha} c(\alpha) \left( 1 - \alpha \sum_{n=1}^{\infty} \frac{d_n(\alpha)}{z^{2n}} \right),$$

$$E_{10}^{\alpha+}(z) = -z^{\alpha-1} c(\alpha) \left( \frac{\alpha}{\alpha+1} \right)^{1/2} \times \left( 1 - \sum_{n=1}^{\infty} \frac{(\alpha-2n)d_n(\alpha)}{z^{2n}} \right),$$

$$E_{11}^{\alpha+}(z) = z^{\alpha-1} \frac{c(\alpha)}{(1+\alpha)} \left( \alpha - \sum_{n=1}^{\infty} \frac{(\alpha-2n)^2 d_n(\alpha)}{z^{2n}} \right), \quad (A1)$$

$$E_{11}^{\alpha-}(z) = -z^{\alpha-2} \frac{c(\alpha)}{(1+\alpha)} \left( (\alpha-1) - \sum_{n=1}^{\infty} \frac{(\alpha-2n)(\alpha-2n-1)d_n(\alpha)}{z^{2n}} \right),$$

where

$$c(\alpha) = 2^{\alpha} \Gamma(\alpha + \frac{1}{2}) / [\pi^{1/2} \Gamma(\alpha + 1)],$$

$$d_n(\alpha) = \frac{2^{-2n} (1-\alpha)(2-\alpha) \cdots (2n-1-\alpha)}{n! (\frac{1}{2}-\alpha)(\frac{3}{2}-\alpha) \cdots (n-\frac{1}{2}-\alpha)}. \quad (A2)$$

<sup>39</sup> F. Cerulus and A. Martin, Phys. Letters **8**, 80 (1964); T. Kinoshita, Phys. Rev. Letters **12**, 257 (1964).

<sup>40</sup> Such a limiting behavior has been suggested from an entirely different point of view by H. D. I. Abarbanel, S. D. Drell, and F. J. Gilman, Phys. Rev. Letters **20**, 280 (1968).

Note that  $c(\alpha)/(1+\alpha)$  is finite at  $\alpha=-1$ . At integer values of  $\alpha$  we have

$$\begin{aligned}
 E_{00}^{\alpha\pm}(z) &= e_{00}^{\alpha\pm}(z) & \text{for } \alpha=0, 1, 2, \dots \\
 &= 0 & \text{for } \alpha=-1, -2, \dots \\
 E_{10}^{\alpha\pm}(z) &= e_{10}^{\alpha\pm}(z) & \text{for } \alpha=0, 1, 2, \dots \\
 &= 0 & \text{for } \alpha=-1, -2, \dots \\
 E_{11}^{\alpha\pm}(z) &= e_{11}^{\alpha\pm}(z) & \text{for } \alpha=1, 2, 3, \dots \\
 &= \text{finite} & \text{for } \alpha=0, -1 \\
 &= 0 & \text{for } \alpha=-2, -3, \dots
 \end{aligned} \tag{A3}$$

These functions have poles at  $\alpha$ =half-integer, with residues satisfying

$$\text{Res}E_{\lambda\mu}^{\alpha\pm} = -\text{Res}E_{\lambda\mu}^{(-\alpha-1)\pm} \text{ at } \alpha = \text{half-integer except } -\frac{1}{2}. \tag{A4}$$

The pole at  $\alpha=-\frac{1}{2}$  is not relevant to our discussion, because it is cancelled by a factor  $\alpha+\frac{1}{2}$  in (36). As (A3) shows,  $E_{11}^{\alpha\pm}$  has the peculiarity that it fails to vanish at the nonsense values  $\alpha=0, -1$ . At these values one can show that

$$E_{11}^{\alpha\pm}(z) = E_{11}^{(-\alpha-1)\mp}(z) \text{ at } \alpha=0, -1. \tag{A5}$$

The symmetries (A4) and (A5), respectively, correspond to (30) and (31) for the partial-wave amplitudes.

Because of the behavior mentioned above, unphysical poles may occur in the scattering amplitudes  $g_i$  of (37), as follows:

- (a) At  $\alpha=\frac{1}{2}, \pm\frac{3}{2}, \pm\frac{5}{2}, \pm\frac{7}{2}, \dots$ , all  $g_i$  may have poles coming from the poles of  $E_{\lambda\mu}^{\alpha\pm}$ .
- (b) At  $\alpha=0, -1$ ,  $g_3$  and  $g_4$  may have poles, because  $\xi(t)$  has a pole at either  $\alpha=0$  or  $\alpha=-1$ , depending on the signature, and  $E_{11}^{\alpha\pm} \neq 0$  at these points.

These poles are in fact absent, for they are always cancelled, either by compensating zeros in  $\beta_{\lambda\mu}^{(i)}$ , or by compensating trajectories, as we have already mentioned.

If compensating trajectories of type (a) occurs, their contributions to  $g_i$  must be added to (36). A compensating trajectory of type (a) will be below the original trajectory  $\alpha$  if  $\alpha > -\frac{1}{2}$ , and above the original trajectory

if  $\alpha < -\frac{1}{2}$ . In the former case its effect is small except in the neighborhood of the point of compensation. In the latter case it will dominate the original trajectory. For simplicity, we assume that the latter case does not happen. Accordingly, we must require  $\beta_{\lambda\mu}=0$  at  $\alpha=-\frac{3}{2}, -\frac{5}{2}, \dots$ . This may be satisfied by putting

$$\begin{aligned}
 \lambda_0(t) &\propto [\Gamma(\alpha(t) + \frac{3}{2})]^{-1}, \\
 \lambda_1(t) &\propto [\Gamma(\alpha(t) + \frac{3}{2})]^{-1},
 \end{aligned} \tag{A6}$$

where  $\lambda_0$  and  $\lambda_1$  are defined in (35).

If compensating trajectories of type (b) occur, their contributions to  $g_i$  must be taken into account through the signatured partial-wave amplitude of opposite parity and signature to the ones considered in (36). To avoid complications that cannot be subjected to unequivocal experimental test in our work, we assume that compensating trajectories of type (b) do not exist. Accordingly, we must require

$$\beta_{11}=0 \text{ at } \alpha=0, -1, \tag{A7}$$

which may be satisfied by putting

$$\lambda_1(t) \propto [\alpha(t)]^2. \tag{A8}$$

The reason for  $\alpha^2$  instead of the simplest choice  $\alpha$  is to avoid introducing a branch point in  $\beta_{10}$  through the factor  $\sqrt{\lambda_1}$ . In our actual fit, in fact, we made the even simpler choice  $\lambda_1 \equiv 0$ , which is of course consistent with (A8).

The choice (A6) and (A8) with no other zeros or poles in  $\lambda_0$  and  $\lambda_1$  corresponds to the dynamical proposal of Chew.<sup>41</sup> We emphasize that it merely represents one out of an infinite number of choices in compensation schemes. So far there is neither theoretically compelling reason nor clear experimental test for the correct scheme.

Even with our choice, the question of compensating trajectories of type (a) for  $\alpha > \frac{1}{2}$  remains open. If they exist, their contributions to the scattering amplitude are of order  $z_i^{-2}$ . To avoid discussing them we neglect terms of this order.

<sup>41</sup> G. F. Chew, Phys. Rev. Letters **16**, 60 (1966). Some other alternatives are discussed in C. B. Chiu, S. Y. Chu, and L. L. Wang, Phys. Rev. **161**, 1563 (1967).